Properties of rotating QCD: current results from lattice simulations

A. A. Roenko,

in collaboration with

V. V. Braguta, A. Yu. Kotov, D. A. Sychev

Joint Institute for Nuclear Research, Bogoliubov Laboratory of Theoretical Physics

Seminar “Theory of Hadronic Matter under Extreme Conditions”, BLTP JINR

Introduction

- In non-central heavy ion collisions creation of QGP with angular momentum is expected.

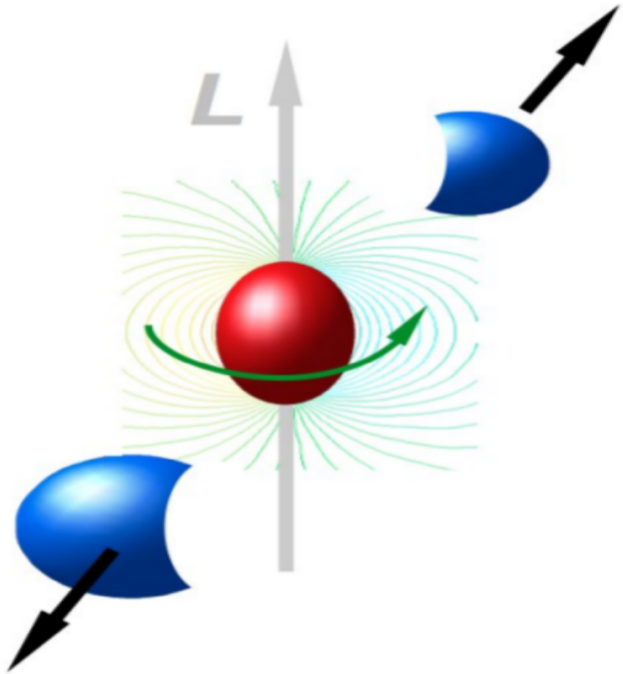

Introduction

- In non-central heavy ion collisions creation of QGP with angular momentum is expected.
- The rotation occurs with relativistic velocities.

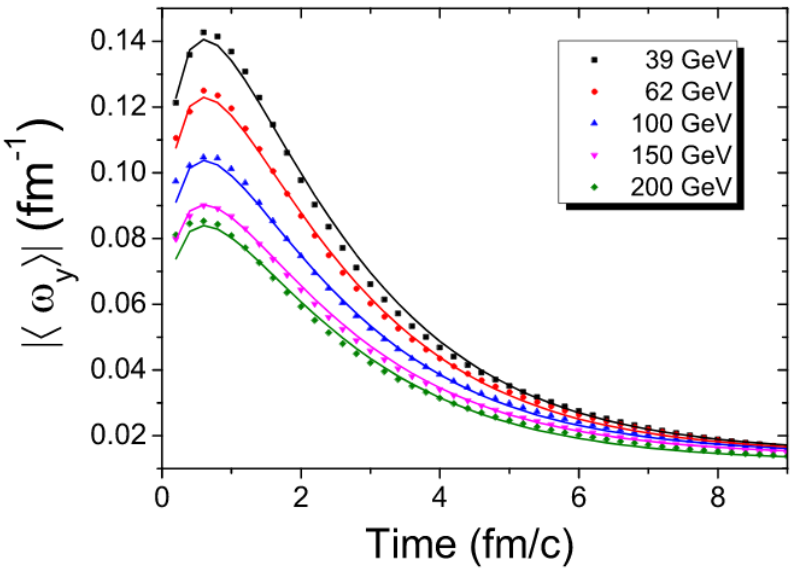

Au+Au, $b = 7$ fm

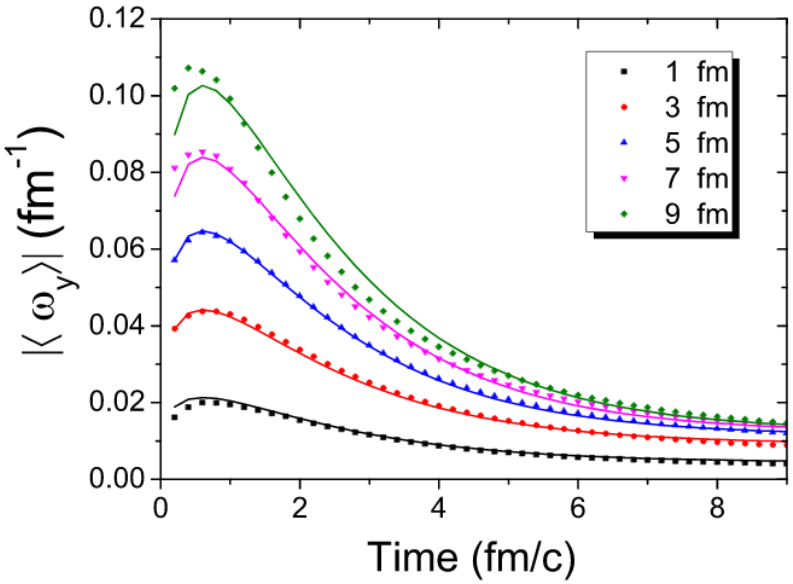

Au+Au, 200 MeV

[Y. Jiang et al., Phys. Rev. C **94**, 044910 (2016), arXiv:1602.06580 [hep-ph]]

$$\omega \sim 0.1 - 0.2\,\mathrm{fm}^{-1} \sim 20 - 40 \ \mathrm{MeV}$$

Introduction

The rotation leads to a number of interesting physical phenomena:

- Chiral Vortical Effect;
  - A. Vilenkin, Phys. Rev. D **20**, 1807–1812 (1979)
  - D. Kharzeev et al., Prog. Part. Nucl. Phys. **88**, 1–28 (2016), arXiv:1511.04050 [hep-ph]
  - G. Y. Prokhorov et al., JHEP **02**, 146 (2019), arXiv:1807.03584 [hep-th]
  - G. Y. Prokhorov et al., Phys. Rev. D **105**, L041701 (2022), arXiv:2109.06048 [hep-th]
  - ...

Introduction

The rotation leads to a number of interesting physical phenomena:

- Chiral Vortical Effect;
- Polarization of various particles;
  - Z.-T. Liang and X.-N. Wang, Phys. Rev. Lett. **94**, [Erratum: Phys.Rev.Lett. 96, 039901 (2006)], 102301 (2005), arXiv:nucl-th/0410079
  - S. A. Voloshin, (2004), arXiv:nucl-th/0410089
  - O. Rogachevsky et al., Phys. Rev. C **82**, 054910 (2010), arXiv:1006.1331 [hep-ph]
  - F. Becattini et al., Phys. Rev. C **88**, [Erratum: Phys.Rev.C 93, 069901 (2016)], 034905 (2013), arXiv:1304.4427 [nucl-th]
  - F. Becattini et al., Phys. Rev. C **95**, 054902 (2017), arXiv:1610.02506 [nucl-th]
  - O. V. Teryaev and V. I. Zakharov, Phys. Rev. D **96**, 096023 (2017)
  - ...

Introduction

The rotation leads to a number of interesting physical phenomena:

- Chiral Vortical Effect;
- Polarization of various particles;

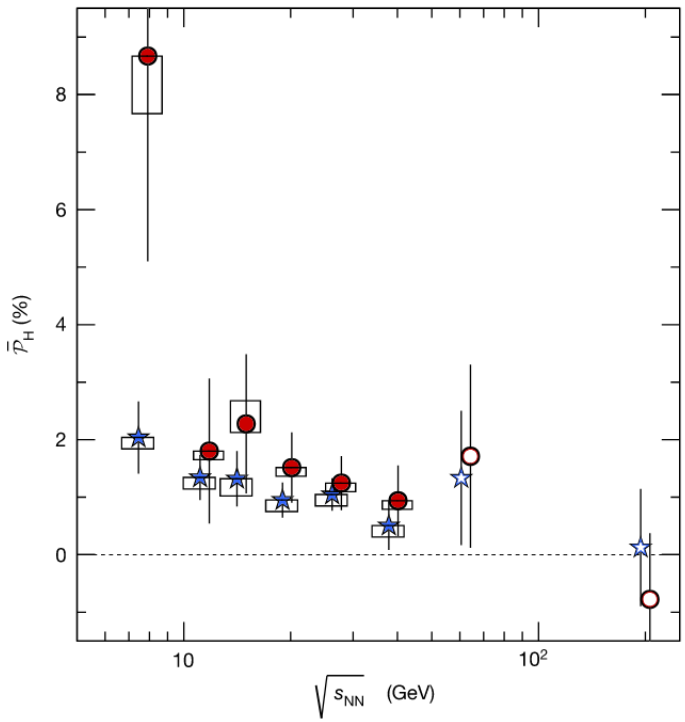

[L. Adamczyk et al. (STAR), Nature **548**, 62–65 (2017), arXiv:1701.06657 [nucl-ex]]

$$\omega \sim 6 \text{ MeV} \quad (\sqrt{s_{NN}}\text{-averaged})$$

- ...
- How does the rotation affect to phase transitions in QCD?

Related papers

Rotation on the lattice (phase transitions were not considered):

- A. Yamamoto and Y. Hirono, Phys. Rev. Lett. **111**, 081601 (2013), arXiv:1303.6292 [hep-lat]

Related papers

Rotation on the lattice (phase transitions were not considered):

- A. Yamamoto and Y. Hirono, Phys. Rev. Lett. **111**, 081601 (2013), arXiv:1303.6292 [hep-lat]

Properties of rotating QCD matter (mostly within NJL, focused on fermions):

- S. M. A. Tabatabaee Mehr and F. Taghinavaz, (2022), arXiv:2201.05398 [hep-ph]
- H. Zhang et al., Chin. Phys. C **44**, 111001 (2020), arXiv:1812.11787 [hep-ph]
- X. Wang et al., Phys. Rev. D **99**, 016018 (2019), arXiv:1808.01931 [hep-ph]
- M. Chernodub and S. Gongyo, JHEP **01**, 136 (2017), arXiv:1611.02598 [hep-th]
- ...
- Y. Jiang and J. Liao, Phys. Rev. Lett. **117**, 192302 (2016), arXiv:1606.03808 [hep-ph]

Related papers

Rotation on the lattice (phase transitions were not considered):

- A. Yamamoto and Y. Hirono, Phys. Rev. Lett. **111**, 081601 (2013), arXiv:1303.6292 [hep-lat]

Properties of rotating QCD matter (mostly within NJL, focused on fermions):

- S. M. A. Tabatabaee Mehr and F. Taghinavaz, (2022), arXiv:2201.05398 [hep-ph]
- H. Zhang et al., Chin. Phys. C **44**, 111001 (2020), arXiv:1812.11787 [hep-ph]
- X. Wang et al., Phys. Rev. D **99**, 016018 (2019), arXiv:1808.01931 [hep-ph]
- M. Chernodub and S. Gongyo, JHEP **01**, 136 (2017), arXiv:1611.02598 [hep-th]
- ...
- Y. Jiang and J. Liao, Phys. Rev. Lett. **117**, 192302 (2016), arXiv:1606.03808 [hep-ph]

Rotation suppress the chiral condensate ($S = 0$), states with $S \neq 0$ are preferable.
$\Rightarrow$ Critical temperature decreases due to the rotation.

Related papers

Rotation on the lattice (phase transitions were not considered):

- A. Yamamoto and Y. Hirono, Phys. Rev. Lett. **111**, 081601 (2013), arXiv:1303.6292 [hep-lat]

Properties of rotating QCD matter (mostly within NJL, focused on fermions):

- S. M. A. Tabatabaee Mehr and F. Taghinavaz, (2022), arXiv:2201.05398 [hep-ph]
- H. Zhang et al., Chin. Phys. C **44**, 111001 (2020), arXiv:1812.11787 [hep-ph]
- X. Wang et al., Phys. Rev. D **99**, 016018 (2019), arXiv:1808.01931 [hep-ph]
- M. Chernodub and S. Gongyo, JHEP **01**, 136 (2017), arXiv:1611.02598 [hep-th]
- ...
- Y. Jiang and J. Liao, Phys. Rev. Lett. **117**, 192302 (2016), arXiv:1606.03808 [hep-ph]

Rotation suppress the chiral condensate ($S = 0$), states with $S \neq 0$ are preferable.
$\Rightarrow$ Critical temperature decreases due to the rotation.

- Holography: N. R. F. Braga et al., Phys. Rev. D **105**, 106003 (2022), arXiv:2201.05581 [hep-th], A. A. Golubtsova et al., Nucl. Phys. B **979**, 115786 (2022), arXiv:2107.11672 [hep-th], X. Chen et al., JHEP **07**, 132 (2021), arXiv:2010.14478 [hep-ph], ...
- Compact QED in 2+1-D M. N. Chernodub, Phys. Rev. D **103**, 054027 (2021), arXiv:2012.04924 [hep-ph]
- HRG model: Y. Fujimoto et al., Phys. Lett. B **816**, 136184 (2021), arXiv:2101.09173 [hep-ph]
- Instantons in rotating YM: M. N. Chernodub, (2022), arXiv:2208.04808 [hep-th]
- Polyakov loop potential in YM with Ω_I (perturbatively, finite T): S. Chen et al., (2022), arXiv:2207.12665 [hep-ph]
- ...

Related papers

The rotation affect both gluon and quark degrees of freedom!

Related papers

The rotation affect both gluon and quark degrees of freedom!

Our lattice results for gluodynamics is opposite: critical temperature increases with rotation.

- V. V. Braguta et al., JETP Lett. **112**, 6–12 (2020)
- V. V. Braguta et al., Phys. Rev. D **103**, 094515 (2021), arXiv:2102.05084 [hep-lat]
- V. Braguta et al., PoS **LATTICE2021**, 125 (2022), arXiv:2110.12302 [hep-lat]

Related papers

The rotation affect both gluon and quark degrees of freedom!

Our lattice results for gluodynamics is opposite: critical temperature increases with rotation.

- V. V. Braguta et al., JETP Lett. **112**, 6–12 (2020)
- V. V. Braguta et al., Phys. Rev. D **103**, 094515 (2021), arXiv:2102.05084 [hep-lat]
- V. Braguta et al., PoS **LATTICE2021**, 125 (2022), arXiv:2110.12302 [hep-lat]

Taking into account the contribution of rotating gluons to NJL model:

- Y. Jiang, (2021), arXiv:2108.09622 [hep-ph]

Related papers

The rotation affect both gluon and quark degrees of freedom!

Our lattice results for gluodynamics is opposite: critical temperature increases with rotation.

- V. V. Braguta et al., JETP Lett. **112**, 6–12 (2020)
- V. V. Braguta et al., Phys. Rev. D **103**, 094515 (2021), arXiv:2102.05084 [hep-lat]
- V. Braguta et al., PoS **LATTICE2021**, 125 (2022), arXiv:2110.12302 [hep-lat]

Taking into account the contribution of rotating gluons to NJL model:

- Y. Jiang, (2021), arXiv:2108.09622 [hep-ph]

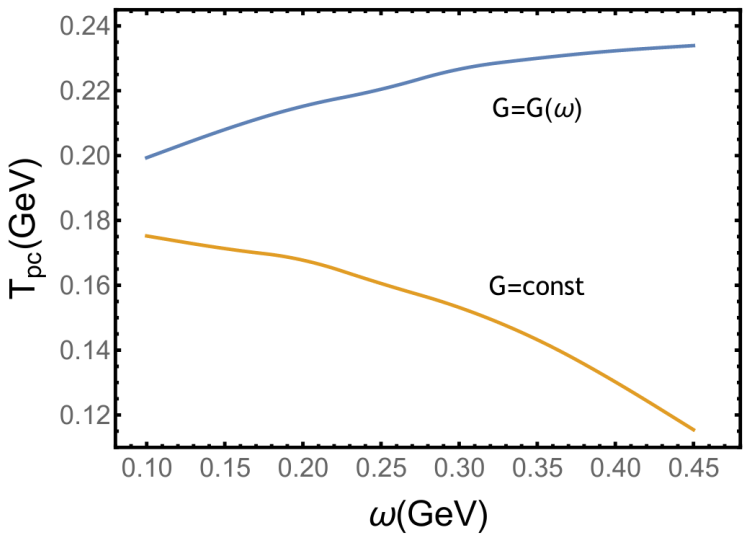

The running effective coupling $G(\omega)$ is introduced.

$\Rightarrow$ Critical temperature increases due to the rotation.

- Rotating QCD in continuum

Rotating reference frame

- QCD (at thermal equilibrium) is investigated in the reference frame which rotates with the system with angular velocity Ω around z-axis.

[1] A. Yamamoto and Y. Hirono, Phys. Rev. Lett. **111**, 081601 (2013), arXiv:1303.6292 [hep-lat].

Rotating reference frame

- QCD (at thermal equilibrium) is investigated in the reference frame which rotates with the system with angular velocity Ω around z-axis.
- In this reference frame there appears an external gravitational field

$$g_{\mu\nu} = \begin{pmatrix} 1 - r^2\Omega^2 & \Omega y & -\Omega x & 0 \\ \Omega y & -1 & 0 & 0 \\ -\Omega x & 0 & -1 & 0 \\ 0 & 0 & 0 & -1 \end{pmatrix} .$$

- The partition function is[1]

$$Z = \int D\psi\, D\bar{\psi}\, DA\, \exp\big(- S_G[A,\Omega] - S_F[\bar{\psi},\psi,A,\Omega]\big) . \qquad (1)$$

The rotation affect both gluon and quark degrees of freedom!

[1] A. Yamamoto and Y. Hirono, Phys. Rev. Lett. **111**, 081601 (2013), arXiv:1303.6292 [hep-lat].

Rotating reference frame

- QCD (at thermal equilibrium) is investigated in the reference frame which rotates with the system with angular velocity Ω around z-axis.
- In this reference frame there appears an external gravitational field

$$g_{\mu\nu} = \begin{pmatrix} 1 - r^2\Omega^2 & \Omega y & -\Omega x & 0 \\ \Omega y & -1 & 0 & 0 \\ -\Omega x & 0 & -1 & 0 \\ 0 & 0 & 0 & -1 \end{pmatrix} .$$

- The partition function is[1]

$$Z = \int D\psi\, D\bar{\psi}\, DA\, \exp\big(- S_G[A,\Omega] - S_F[\bar{\psi},\psi,A,\Omega]\big) . \qquad (1)$$

The rotation affect both gluon and quark degrees of freedom!

Interplay between these effects may lead to non-trivial results.

[1] A. Yamamoto and Y. Hirono, Phys. Rev. Lett. **111**, 081601 (2013), arXiv:1303.6292 [hep-lat].

The Euclidean gluon action can be written as

$$S_G = \frac{1}{4g^2}\int d^4x\,\sqrt{g_E}\,g_E^{\mu\nu}\,g_E^{\alpha\beta}\,F^a_{\mu\alpha}F^a_{\nu\beta}\,. \tag{2}$$

And the quark action reads as follows[2]

$$S_F = \int d^4x\,\sqrt{g_E}\,\bar{\psi}\big(\gamma^\mu(D_\mu - \Gamma_\mu) + m\big)\psi\,, \tag{3}$$

The covariant derivative D_μ and spinor affine connection Γ_μ is

$$D_\mu = \partial_\mu - iA_\mu\,, \tag{4}$$

$$\Gamma_\mu = -\frac{i}{4}\sigma^{ij}\omega_{\mu ij}\,, \tag{5}$$

$$\sigma^{ij} = \frac{i}{2}(\gamma^i\gamma^j - \gamma^j\gamma^i) \tag{6}$$

$$\omega_{\mu ij} = g^E_{\alpha\beta}e^\alpha_i(\partial_\mu e^\beta_j + \Gamma^\beta_{\nu\mu}e^\nu_j) \tag{7}$$

where e^μ_i is the vierbein and $\Gamma^\alpha_{\mu\nu}$ is the Christoffel symbol.

[2] A. Yamamoto and Y. Hirono, Phys. Rev. Lett. **111**, 081601 (2013), arXiv:1303.6292 [hep-lat].

The Euclidean metric tensor can be obtained from $g_{\mu\nu}$ by Wick rotation $t \to i\tau$

$$g^E_{\mu\nu} = \begin{pmatrix} 1 & 0 & 0 & y\Omega_I \\ 0 & 1 & 0 & -x\Omega_I \\ 0 & 0 & 1 & 0 \\ y\Omega_I & -x\Omega_I & 0 & 1 + r^2\Omega_I^2 \end{pmatrix},$$

where imaginary angular velocity $\Omega_I = -i\Omega$ is introduced.

The Euclidean metric tensor can be obtained from $g_{\mu\nu}$ by Wick rotation $t \to i\tau$

$$g^E_{\mu\nu} = \begin{pmatrix} 1 & 0 & 0 & y\Omega_I \\ 0 & 1 & 0 & -x\Omega_I \\ 0 & 0 & 1 & 0 \\ y\Omega_I & -x\Omega_I & 0 & 1 + r^2\Omega_I^2 \end{pmatrix},$$

where imaginary angular velocity $\Omega_I = -i\Omega$ is introduced. Substituting the $(g_E)_{\mu\nu}$ to formula (8) one gets

$$S_G = \frac{1}{2g^2}\int d^4x \Big[(1 + r^2\Omega_I^2)F^a_{xy}F^a_{xy} + (1 + y^2\Omega_I^2)F^a_{xz}F^a_{xz} + (1 + x^2\Omega_I^2)F^a_{yz}F^a_{yz} +$$
$$+ F^a_{x\tau}F^a_{x\tau} + F^a_{y\tau}F^a_{y\tau} + F^a_{z\tau}F^a_{z\tau} -$$
$$+ 2y\Omega_I(F^a_{xy}F^a_{y\tau} + F^a_{xz}F^a_{z\tau}) - 2x\Omega_I(F^a_{yx}F^a_{x\tau} + F^a_{yz}F^a_{z\tau}) + 2xy\Omega_I^2F^a_{xz}F^a_{zy}\Big].$$

Rotating QCD

The Euclidean metric tensor can be obtained from $g_{\mu\nu}$ by Wick rotation $t \to i\tau$

$$g^E_{\mu\nu} = \begin{pmatrix} 1 & 0 & 0 & y\Omega_I \\ 0 & 1 & 0 & -x\Omega_I \\ 0 & 0 & 1 & 0 \\ y\Omega_I & -x\Omega_I & 0 & 1 + r^2\Omega_I^2 \end{pmatrix},$$

where imaginary angular velocity $\Omega_I = -i\Omega$ is introduced. Substituting the $(g_E)_{\mu\nu}$ to formula (8) one gets

$$S_G = \frac{1}{2g^2}\int d^4x \Big[(1 + r^2\Omega_I^2)F^a_{xy}F^a_{xy} + (1 + y^2\Omega_I^2)F^a_{xz}F^a_{xz} + (1 + x^2\Omega_I^2)F^a_{yz}F^a_{yz} +$$
$$+ F^a_{x\tau}F^a_{x\tau} + F^a_{y\tau}F^a_{y\tau} + F^a_{z\tau}F^a_{z\tau} -$$
$$+ 2y\Omega_I(F^a_{xy}F^a_{y\tau} + F^a_{xz}F^a_{z\tau}) - 2x\Omega_I(F^a_{yx}F^a_{x\tau} + F^a_{yz}F^a_{z\tau}) + 2xy\Omega_I^2F^a_{xz}F^a_{zy}\Big].$$

Sign problem

- The Euclidean action is complex-valued function with real rotation!
- The Monte–Carlo simulations are conducted with imaginary angular velocity $\Omega_I = -i\Omega$.
- The results are analytically continued to the region of the real angular velocity.

The covariant Dirac operator depends on the choice of the vierbein. We choose the vierbein in the form

$$e_1^x = e_2^y = e_3^z = e_4^\tau = 1\,, \quad e_4^x = -y\Omega_I\,, \quad e_4^y = x\Omega_i\,, \quad \text{and other } e_i^\mu = 0$$

As the result, the Euclidean quark action is

$$S_F = \int d^4x\,\bar{\psi}\left(\gamma^x D_x + \gamma^x D_x + \gamma^x D_x + \gamma^\tau\left(D_\tau + i\Omega_I\frac{\sigma^{12}}{2}\right) + m\right)\psi\,, \tag{8}$$

where the gamma matrices are given by $\gamma^\mu = \gamma^i e_i^\mu$

$$\gamma^x = \gamma^1 - y\Omega_I\gamma^4\,, \quad \gamma^y = \gamma^2 + x\Omega_I\gamma^4\,, \quad \gamma^z = \gamma^3\,, \quad \gamma^\tau = \gamma^4\,. \tag{9}$$

The covariant Dirac operator depends on the choice of the vierbein. We choose the vierbein in the form

$$e_1^x = e_2^y = e_3^z = e_4^\tau = 1\,, \quad e_4^x = -y\Omega_I\,, \quad e_4^y = x\Omega_i\,, \quad \text{and other } e_i^\mu = 0$$

As the result, the Euclidean quark action is

$$S_F = \int d^4x\,\bar{\psi}\left(\gamma^x D_x + \gamma^x D_x + \gamma^x D_x + \gamma^\tau\left(D_\tau + i\Omega_I\frac{\sigma^{12}}{2}\right) + m\right)\psi\,, \tag{8}$$

where the gamma matrices are given by $\gamma^\mu = \gamma^i e_i^\mu$

$$\gamma^x = \gamma^1 - y\Omega_I\gamma^4\,, \quad \gamma^y = \gamma^2 + x\Omega_I\gamma^4\,, \quad \gamma^z = \gamma^3\,, \quad \gamma^\tau = \gamma^4\,. \tag{9}$$

The quark action contains orbit-rotation coupling term $\gamma^\tau\Omega_I(xD_y - yD_x)$ and spin-rotation coupling term $i\gamma^\tau\Omega_I\sigma^{12}/2$.

The covariant Dirac operator depends on the choice of the vierbein. We choose the vierbein in the form

$$e_1^x = e_2^y = e_3^z = e_4^\tau = 1\,, \quad e_4^x = -y\Omega_I\,, \quad e_4^y = x\Omega_i\,, \quad \text{and other } e_i^\mu = 0$$

As the result, the Euclidean quark action is

$$S_F = \int d^4x\,\bar{\psi}\left(\gamma^x D_x + \gamma^x D_x + \gamma^x D_x + \gamma^\tau\left(D_\tau + i\Omega_I\frac{\sigma^{12}}{2}\right) + m\right)\psi\,, \tag{8}$$

where the gamma matrices are given by $\gamma^\mu = \gamma^i e_i^\mu$

$$\gamma^x = \gamma^1 - y\Omega_I\gamma^4\,, \quad \gamma^y = \gamma^2 + x\Omega_I\gamma^4\,, \quad \gamma^z = \gamma^3\,, \quad \gamma^\tau = \gamma^4\,. \tag{9}$$

The quark action contains orbit-rotation coupling term $\gamma^\tau\Omega_I(xD_y - yD_x)$ and spin-rotation coupling term $i\gamma^\tau\Omega_I\sigma^{12}/2$.

Sign problem

- The Euclidean action is complex-valued function with real rotation!

Rotating reference frame: temperature

$$\int d^4x\sqrt{g_E}\,(\dots) = \int_0^{1/T} dx_0\sqrt{g_{44}}\int d^3x\sqrt{\gamma_E}\,(\dots) = \int_0^{1/T} dx_0\int d^3x\sqrt{g_E}\,(\dots)$$

- Interpretation: Tolman-Ehrenfest effect. In gravitational field the temperature isn't a constant in space at thermal equilibrium:

$$T(r)\sqrt{g_{00}} = const\,,$$

Rotating reference frame: temperature

$$\int d^4x\sqrt{g_E}\,(\dots) = \int_0^{1/T} dx_0\sqrt{g_{44}}\int d^3x\sqrt{\gamma_E}\,(\dots) = \int_0^{1/T} dx_0\int d^3x\sqrt{g_E}\,(\dots)$$

- Interpretation: Tolman-Ehrenfest effect. In gravitational field the temperature isn't a constant in space at thermal equilibrium:

$$T(r)\sqrt{g_{00}} = const\,,$$

- For the (real) rotation one has

$$T(r)\sqrt{1-r^2\Omega^2} = const \equiv T\,,$$

- One could expect, that the rotation effectively warm up the periphery of the modeling volume

$$T(r) > T(r=0),$$

and as a result, from kinematics, the critical temperature should decreases.

- Rotating QCD on the lattice

Rotating QCD: gluon lattice action

The (improved) lattice gluon action can be written as

$$S_G = \beta \sum_x \Big((c_0 + r^2\Omega_I^2) W_{xy}^{1\times 1} + (c_0 + y^2\Omega_I^2) W_{xz}^{1\times 1} + (c_0 + x^2\Omega_I^2) W_{yz}^{1\times 1} + \\ + c_0 \left(W_{x\tau}^{1\times 1} + W_{y\tau}^{1\times 1} + W_{z\tau}^{1\times 1} \right) + y\Omega_I \left(W_{xy\tau}^{1\times 1\times 1} + W_{xz\tau}^{1\times 1\times 1} \right) - \\ - x\Omega_I \left(W_{yx\tau}^{1\times 1\times 1} + W_{yz\tau}^{1\times 1\times 1} \right) + xy\Omega_I^2 W_{xzy}^{1\times 1\times 1} + \sum_{\mu\neq\nu} c_1 W_{\mu\nu}^{1\times 2} \Big) , \quad (10)$$

with $\beta = 6/g^2$, and $c_0 = 1 - 8c_1$, where

$$W_{\mu\nu}^{1\times 1}(x) = 1 - \frac{1}{3}\text{Re Tr } \bar{U}_{\mu\nu}(x) , \quad (11)$$

$$W_{\mu\nu}^{1\times 2}(x) = 1 - \frac{1}{3}\text{Re Tr } R_{\mu\nu}(x) , \quad (12)$$

$$W_{\mu\nu\rho}^{1\times 1\times 1}(x) = -\frac{1}{3}\text{Re Tr } \bar{V}_{\mu\nu\rho}(x) , \quad (13)$$

$\bar{U}_{\mu\nu}$ denotes clover-type average of 4 plaquettes,

$R_{\mu\nu}$ is a rectangular loop,

$\bar{V}_{\mu\nu\rho}$ is asymmetric chair-type average of 8 chairs.

Rotating QCD: gluon lattice action

The (improved) lattice gluon action can be written as

$$S_G = \beta \sum_x \Big((c_0 + r^2\Omega_I^2) W_{xy}^{1\times 1} + (c_0 + y^2\Omega_I^2) W_{xz}^{1\times 1} + (c_0 + x^2\Omega_I^2) W_{yz}^{1\times 1} + \\ + c_0 \left(W_{x\tau}^{1\times 1} + W_{y\tau}^{1\times 1} + W_{z\tau}^{1\times 1} \right) + y\Omega_I \left(W_{xy\tau}^{1\times 1\times 1} + W_{xz\tau}^{1\times 1\times 1} \right) - \\ - x\Omega_I \left(W_{yx\tau}^{1\times 1\times 1} + W_{yz\tau}^{1\times 1\times 1} \right) + xy\Omega_I^2 W_{xzy}^{1\times 1\times 1} + \sum_{\mu\neq\nu} c_1 W_{\mu\nu}^{1\times 2} \Big) , \quad (10)$$

with $\beta = 6/g^2$, and $c_0 = 1 - 8c_1$, where

$$W_{\mu\nu}^{1\times 1}(x) = 1 - \frac{1}{3}\text{Re Tr } \bar{U}_{\mu\nu}(x) , \quad (11)$$

$$W_{\mu\nu}^{1\times 2}(x) = 1 - \frac{1}{3}\text{Re Tr } R_{\mu\nu}(x) , \quad (12)$$

$$W_{\mu\nu\rho}^{1\times 1\times 1}(x) = -\frac{1}{3}\text{Re Tr } \bar{V}_{\mu\nu\rho}(x) , \quad (13)$$

$\bar{U}_{\mu\nu}$ denotes clover-type average of 4 plaquettes,

$R_{\mu\nu}$ is a rectangular loop,

$\bar{V}_{\mu\nu\rho}$ is asymmetric chair-type average of 8 chairs.

Rotating QCD: gluon lattice action

The (improved) lattice gluon action can be written as

$$S_G = \beta \sum_x \Big((c_0 + r^2\Omega_I^2) W_{xy}^{1\times 1} + (c_0 + y^2\Omega_I^2) W_{xz}^{1\times 1} + (c_0 + x^2\Omega_I^2) W_{yz}^{1\times 1} + \\ + c_0 \left(W_{x\tau}^{1\times 1} + W_{y\tau}^{1\times 1} + W_{z\tau}^{1\times 1} \right) + y\Omega_I \left(W_{xy\tau}^{1\times 1\times 1} + W_{xz\tau}^{1\times 1\times 1} \right) - \\ - x\Omega_I \left(W_{yx\tau}^{1\times 1\times 1} + W_{yz\tau}^{1\times 1\times 1} \right) + xy\Omega_I^2 W_{xzy}^{1\times 1\times 1} + \sum_{\mu\neq\nu} c_1 W_{\mu\nu}^{1\times 2} \Big) , \quad (10)$$

with $\beta = 6/g^2$, and $c_0 = 1 - 8c_1$, where

$$W_{\mu\nu}^{1\times 1}(x) = 1 - \frac{1}{3}\mathrm{Re\ Tr}\ \bar{U}_{\mu\nu}(x) , \quad (11)$$

$$W_{\mu\nu}^{1\times 2}(x) = 1 - \frac{1}{3}\mathrm{Re\ Tr}\ R_{\mu\nu}(x) , \quad (12)$$

$$W_{\mu\nu\rho}^{1\times 1\times 1}(x) = -\frac{1}{3}\mathrm{Re\ Tr}\ \bar{V}_{\mu\nu\rho}(x) , \quad (13)$$

$c_1 = 0$ – Wilson gauge action;

$c_1 = -0.331$ – tree-level improved (Symanzik) gauge action;

$c_1 = -1/12$ – RG-improved (Iwasaki) gauge action;

Rotating QCD: quark lattice action

The lattice quark action has the following form ($N_f = 2$ clover-improved Wilson fermions are used)

$$S_F = \sum_f \sum_{x_1,x_2} \bar{\psi}^f(x_1) \Big\{ \delta_{x_1,x_2} - \kappa \Big[(1-\gamma^x) T_{x+} + (1+\gamma^x) T_{x-} + (1-\gamma^y) T_{y+} + (1+\gamma^y) T_{y-} + (1-\gamma^z) T_{z+} + (1+\gamma^z) T_{z-} + (1-\gamma^\tau) \exp\left(ia\Omega_I \frac{\sigma^{12}}{2} \right) T_{\tau+} + (1+\gamma^\tau) \exp\left(-ia\Omega_I \frac{\sigma^{12}}{2} \right) T_{\tau-} \Big] - \delta_{x_1,x_2} c_{SW} \kappa \sum_{\mu<\nu} \sigma_{\mu\nu} F_{\mu\nu} \Big\} \psi^f(x_2), \quad (14)$$

where $\kappa = 1/(8+2am)$, $T_{\mu+} = U_\mu(x_1)\delta_{x_1+\mu,x_2}$, $T_{\mu-} = U_\mu^\dagger(x_1)\delta_{x_1-\mu,x_2}$ and

$$\gamma^x = \gamma^1 - y\Omega_I\gamma^4, \quad \gamma^y = \gamma^2 + x\Omega_I\gamma^4, \quad \gamma^z = \gamma^3, \quad \gamma^\tau = \gamma^4.$$

The spin-rotation coupling term is exponentiated like chemical potential.

The clover coefficient is taken as $c_{SW} = (1 - W^{1\times1})^{-3/4} = (1 - 0.8412/\beta)^{-3/4}$ (one-loop result for the plaquette are used).

Rotating QCD: quark lattice action

The lattice quark action has the following form ($N_f = 2$ clover-improved Wilson fermions are used)

$$S_F = \sum_f \sum_{x_1,x_2} \bar{\psi}^f(x_1) \Big\{ \delta_{x_1,x_2} - \kappa \Big[(1-\gamma^x) T_{x+} + (1+\gamma^x) T_{x-} + (1-\gamma^y) T_{y+} + (1+\gamma^y) T_{y-} + (1-\gamma^z) T_{z+} + (1+\gamma^z) T_{z-} + (1-\gamma^\tau) \exp\left(ia\Omega_I \frac{\sigma^{12}}{2} \right) T_{\tau+} + (1+\gamma^\tau) \exp\left(-ia\Omega_I \frac{\sigma^{12}}{2} \right) T_{\tau-} \Big] - \delta_{x_1,x_2} c_{SW} \kappa \sum_{\mu<\nu} \sigma_{\mu\nu} F_{\mu\nu} \Big\} \psi^f(x_2), \quad (14)$$

where $\kappa = 1/(8+2am)$, $T_{\mu+} = U_\mu(x_1)\delta_{x_1+\mu,x_2}$, $T_{\mu-} = U_\mu^\dagger(x_1)\delta_{x_1-\mu,x_2}$ and

$$\gamma^x = \gamma^1 - y\Omega_I\gamma^4, \quad \gamma^y = \gamma^2 + x\Omega_I\gamma^4, \quad \gamma^z = \gamma^3, \quad \gamma^\tau = \gamma^4.$$

The spin-rotation coupling term is exponentiated like chemical potential.

The clover coefficient is taken as $c_{SW} = (1 - W^{1\times1})^{-3/4} = (1 - 0.8412/\beta)^{-3/4}$ (one-loop result for the plaquette are used).

Lattice setup

The resulting partition function is

$$Z = \int D\psi\, D\bar{\psi}\, DU\, \exp\big(- S_G[U, \Omega_I] - S_F[\bar{\psi}, \psi, m, U, \Omega_I]\big) =$$

$$= \int DU\, \det M[m, U, \Omega_I]\, e^{(-S_G[U,\Omega_I])} \quad (15)$$

- The rotation affect both gluon and quark degrees of freedom!

Lattice setup

The resulting partition function is

$$Z = \int D\psi\, D\bar{\psi}\, DU\, \exp\big(-S_G[U,\Omega_I] - S_F[\bar{\psi},\psi,m,U,\Omega_I]\big) = \\ = \int DU\, \det M[m,U,\Omega_I]\, e^{(-S_G[U,\Omega_I])} \quad (15)$$

- The rotation affect both gluon and quark degrees of freedom!
- Simulation is performed on the lattice $N_t \times N_z \times N_s^2$ $(N_s = N_x = N_y)$, which rotates around z-axis.

Lattice setup

The resulting partition function is

$$Z = \int D\psi\, D\bar{\psi}\, DU\, \exp\big(-S_G[U,\Omega_I] - S_F[\bar{\psi},\psi,m,U,\Omega_I]\big) = \\ = \int DU\, \det M[m,U,\Omega_I]\, e^{(-S_G[U,\Omega_I])} \quad (15)$$

- The rotation affect both gluon and quark degrees of freedom!
- Simulation is performed on the lattice $N_t \times N_z \times N_s^2$ $(N_s = N_x = N_y)$, which rotates around z-axis.
- $g_{00} = \sqrt{1 - r^2\Omega^2}$ $\Rightarrow$ The system should be limited in the directions, which are orthogonal to the rotation axis: $\Omega_I(N_s - 1)a/\sqrt{2} < 1$

Lattice setup

The resulting partition function is

$$Z = \int D\psi\, D\bar{\psi}\, DU\, \exp\big(-S_G[U,\Omega_I] - S_F[\bar{\psi},\psi,m,U,\Omega_I]\big) = \\ = \int DU\, \det M[m,U,\Omega_I]\, e^{(-S_G[U,\Omega_I])} \quad (15)$$

- The rotation affect both gluon and quark degrees of freedom!
- Simulation is performed on the lattice $N_t \times N_z \times N_s^2$ $(N_s = N_x = N_y)$, which rotates around z-axis.
- $g_{00} = \sqrt{1 - r^2\Omega^2}$ $\Rightarrow$ The system should be limited in the directions, which are orthogonal to the rotation axis: $\Omega_I(N_s - 1)a/\sqrt{2} < 1$

$$\Downarrow$$

- The boundary conditions in directions x, y have to be treated carefully! The results depend on BC for any approach. (PBC are used in directions t, z.)

Lattice setup

The resulting partition function is

$$Z = \int D\psi\, D\bar{\psi}\, DU\, \exp\big(-S_G[U,\Omega_I] - S_F[\bar{\psi},\psi,m,U,\Omega_I]\big) = \\ = \int DU\, \det M[m,U,\Omega_I]\, e^{(-S_G[U,\Omega_I])} \quad (15)$$

- The rotation affect both gluon and quark degrees of freedom!
- Simulation is performed on the lattice $N_t \times N_z \times N_s^2$ $(N_s = N_x = N_y)$, which rotates around z-axis.
- $g_{00} = \sqrt{1 - r^2\Omega^2}$ $\Rightarrow$ The system should be limited in the directions, which are orthogonal to the rotation axis: $\Omega_I(N_s - 1)a/\sqrt{2} < 1$

$$\Downarrow$$

- The boundary conditions in directions x, y have to be treated carefully! The results depend on BC for any approach. (PBC are used in directions t, z.)
- $g_{44} = \sqrt{1 + r^2\Omega_I^2}$ $\Rightarrow$ There is no coordinate singularity in the Euclidean rotation (but the local velocity should be small for the analytic continuation)

- Critical temperature in SU(3) gluodynamics

Rotating gluodynamics: lattice setup

- Wilson gauge action ($c_1 = 0$)

Rotating gluodynamics: lattice setup

- Wilson gauge action ($c_1 = 0$)

The following types of BC were systematically checked:

- Open b.c. – OBC
  - All $U_{\mu\nu}$, $V_{\mu\nu\rho}$, which contain links sticking out of the lattice, excluded.
  - Does not break any symmetries.
  - $U_P = 1$ for all $P \in$ out; or $F_{\mu\nu} = 0 \quad \Rightarrow \quad$ „low“ temperature on the boundary.
- Periodic b.c. – PBC
  - The velocity distribution is not periodic.

Rotating gluodynamics: lattice setup

- Wilson gauge action ($c_1 = 0$)

The following types of BC were systematically checked:

- Open b.c. – OBC
  - All $U_{\mu\nu}$, $V_{\mu\nu\rho}$, which contain links sticking out of the lattice, excluded.
  - Does not break any symmetries.
  - $U_P = 1$ for all $P \in$ out; or $F_{\mu\nu} = 0 \quad \Rightarrow \quad$ „low“ temperature on the boundary.
- Periodic b.c. – PBC
  - The velocity distribution is not periodic.
- Dirichlet b.c. – DBC
  - $U_\mu(x) = \hat{1}$ for all $x, x + \mu \in$ boundary
  - Violate $\mathbb{Z}_3$ center symmetry.
  - $L(x, y) = 3$ on the boundary $\quad \Rightarrow \quad$ „high“ temperature on the boundary.

Rotating gluodynamics: critical temperature

The Polyakov loop is an order parameter. The lattice version is defined as usual:

$$L(\vec{x}) = \mathrm{Tr}\left[\prod_{\tau=0}^{N_t-1} U_4(\vec{x},\tau)\right], \qquad L = \frac{1}{N_s^2 N_z}\sum_{\vec{x}} L(\vec{x})\,. \tag{16}$$

In confinement $\langle L\rangle = 0$; in deconfinement $\langle L\rangle \neq 0$ ($\mathbb{Z}_3$ center symmetry is broken).

The critical temperature T_c is determined using the Polyakov loop susceptibility

$$\chi = N_s^2 N_z \left(\langle |L|^2\rangle - \langle |L|\rangle^2\right), \tag{17}$$

by means of the Gaussian fit.

Rotating gluodynamics: critical temperature

The Polyakov loop is an order parameter. The lattice version is defined as usual:

$$L(\vec{x}) = \mathrm{Tr}\left[\prod_{\tau=0}^{N_t-1} U_4(\vec{x},\tau)\right], \qquad L = \frac{1}{N_s^2 N_z}\sum_{\vec{x}} L(\vec{x})\,. \tag{16}$$

In confinement $\langle L\rangle = 0$; in deconfinement $\langle L\rangle \neq 0$ ($\mathbb{Z}_3$ center symmetry is broken).

The critical temperature T_c is determined using the Polyakov loop susceptibility

$$\chi = N_s^2 N_z \left(\langle |L|^2\rangle - \langle |L|\rangle^2\right), \tag{17}$$

by means of the Gaussian fit.

- Non-periodic b.c. changes the critical temperature $T_c(0)$
  - $T_c(0)^{OBC} > T_c(0)^{PBC}$
  - $T_c(0)^{DBC} < T_c(0)^{PBC}$
- With $N_s/N_t \to \infty$ their influence wanes, and $T_c(0) \to T_c(0)^{(PBC)}$
- The spatial distributions of the local Polyakov loop $L(x,y) = \frac{1}{N_z}\sum_z L(x,y,z)$ show that the boundary is screened.

Rotating gluodynamics: Open boundary conditions

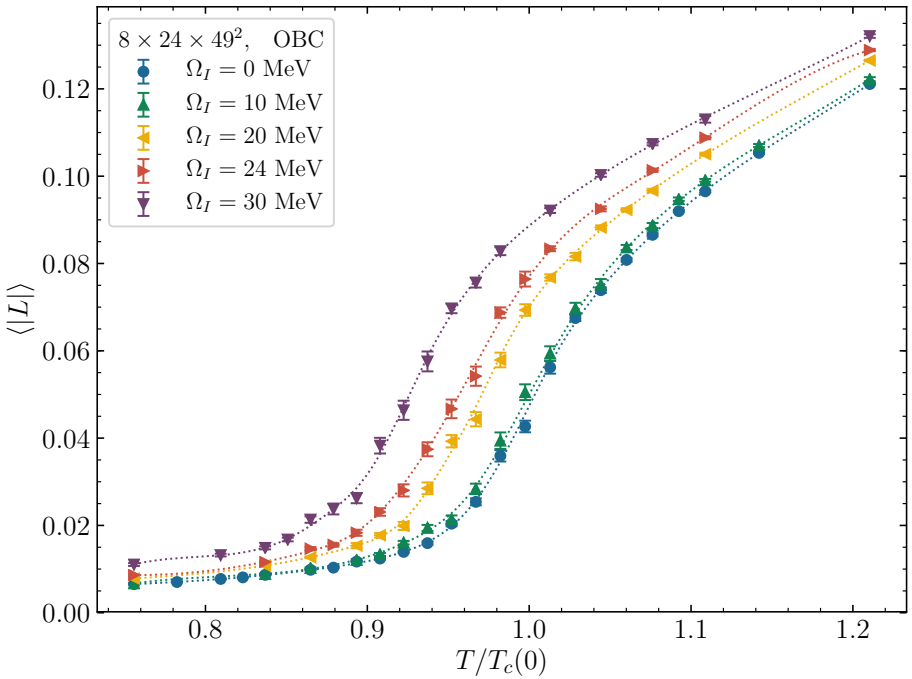

(a)

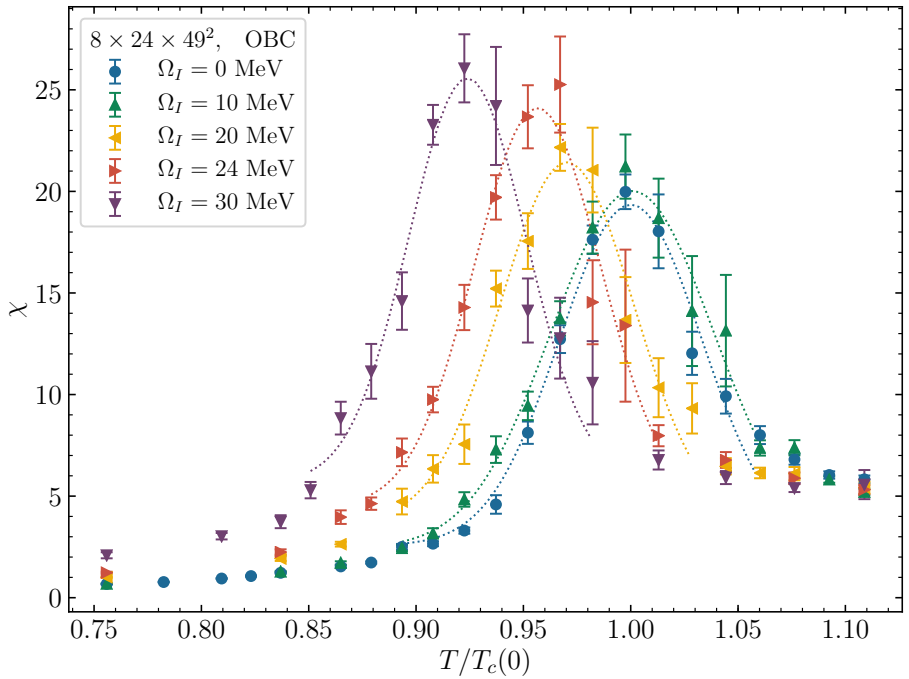

(b)

Figure: The Polyakov loop (a) and Polyakov loop susceptibility (b) as a function of temperature for different values of imaginary angular velocity Ω_I. The results are obtained on the lattice $8 \times 24 \times 49^2$.

Rotating gluodynamics: Open boundary conditions

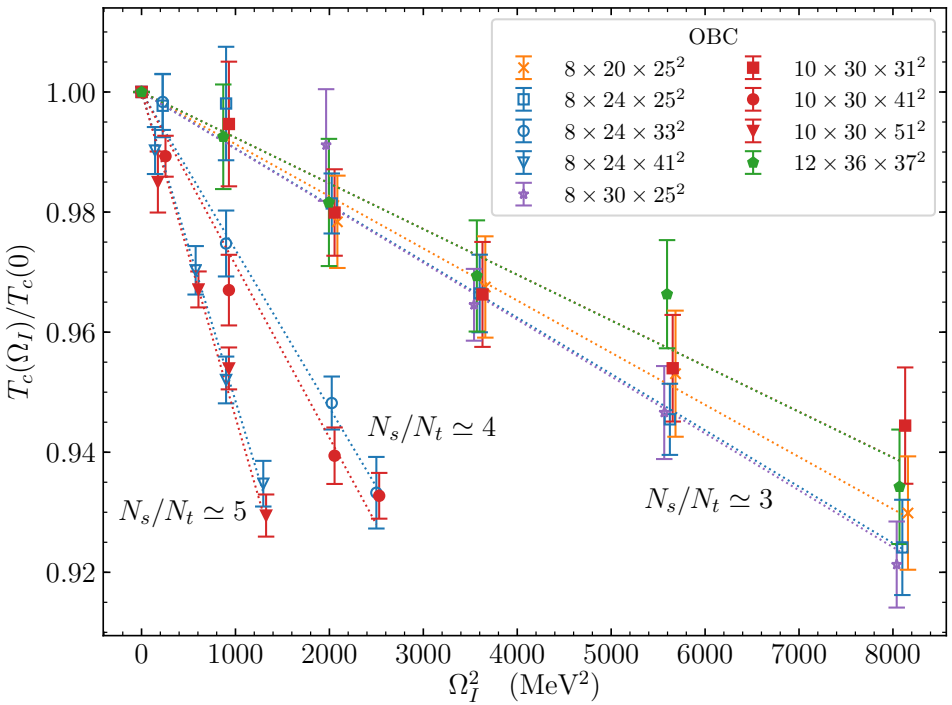

T_c depends on Ω_I^2 and is well described by

$$\frac{T_c(\Omega_I)}{T_c(0)} = 1 - C_2 \Omega_I^2$$

- The coefficient C_2 depends on the transverse lattice size (N_s/N_t) and is almost independent of both the lattice spacing and the lattice size along the rotation axis (N_z/N_t).

Rotating gluodynamics: Open boundary conditions

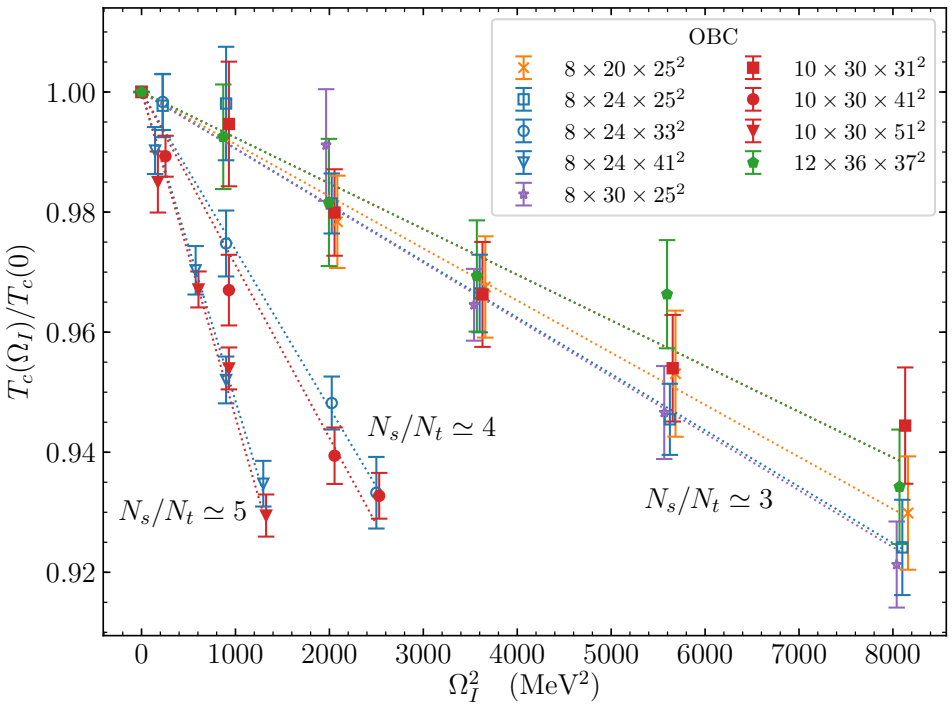

T_c depends on Ω_I^2 and is well described by

$$\frac{T_c(\Omega_I)}{T_c(0)} = 1 - C_2\Omega_I^2$$

$$\Downarrow \quad (\Omega_I^2 = -\Omega^2)$$

$$\frac{T_c(\Omega)}{T_c(0)} = 1 + C_2\Omega^2$$

The critical temperature increases with the angular velocity ($C_2 > 0$)

- The coefficient C_2 depends on the transverse lattice size (N_s/N_t) and is almost independent of both the lattice spacing and the lattice size along the rotation axis (N_z/N_t).

Rotating gluodynamics: Open boundary conditions

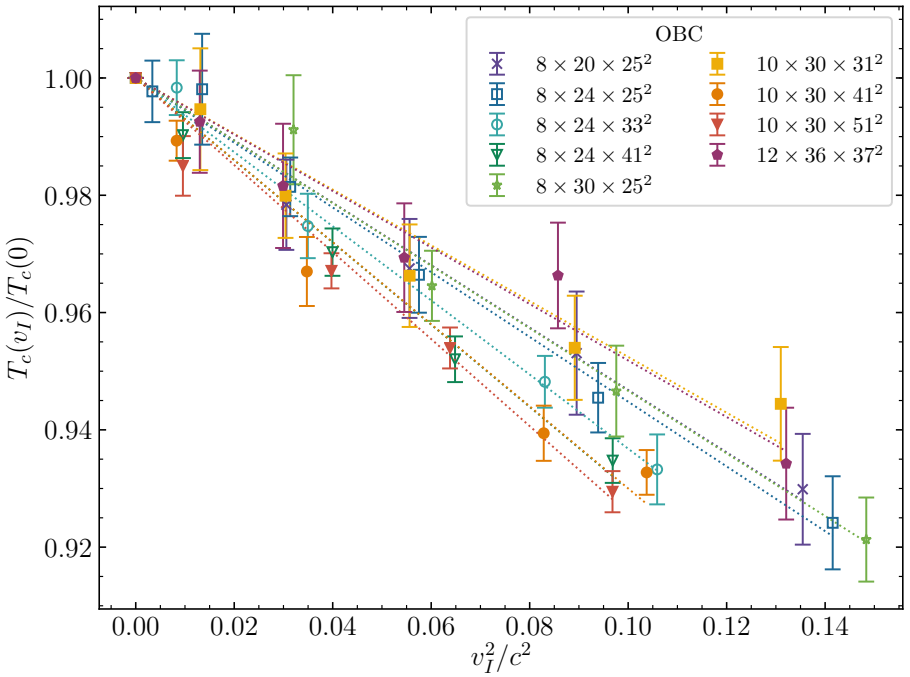

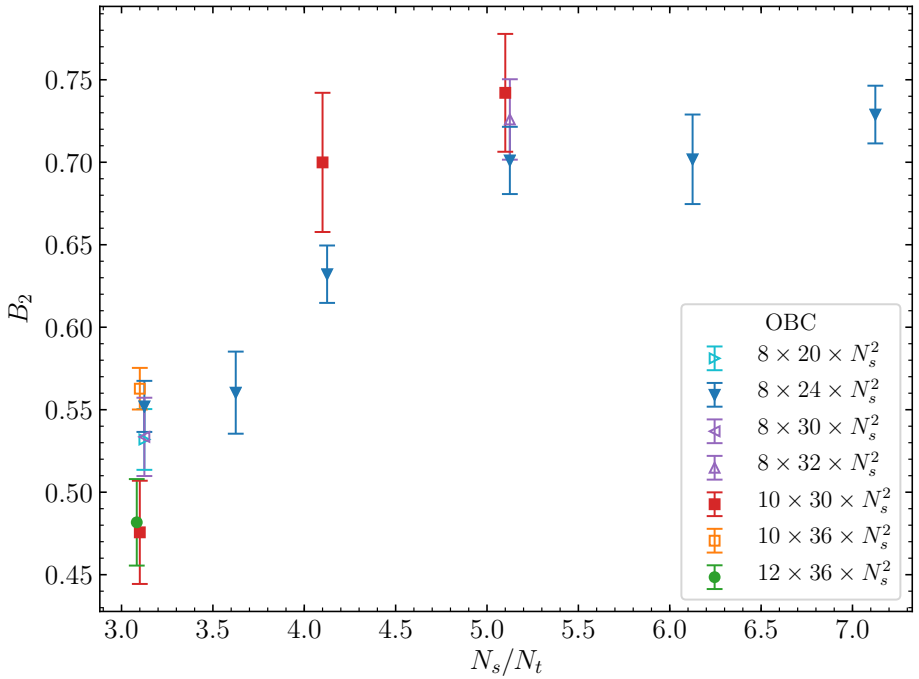

The linear velocity on the boundary $v_I = \Omega_I \, (N_s - 1) \, a(\beta_c)/2$

$$\frac{T_c(v_I)}{T_c(0)} = 1 - B_2 \frac{v_I^2}{c^2}$$

Rotating gluodynamics: Open boundary conditions

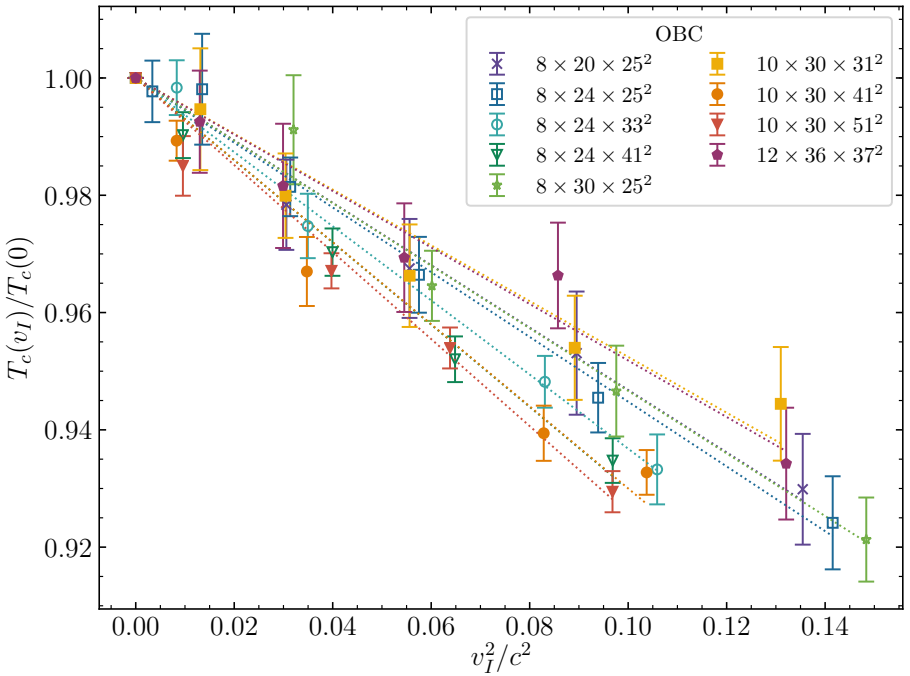

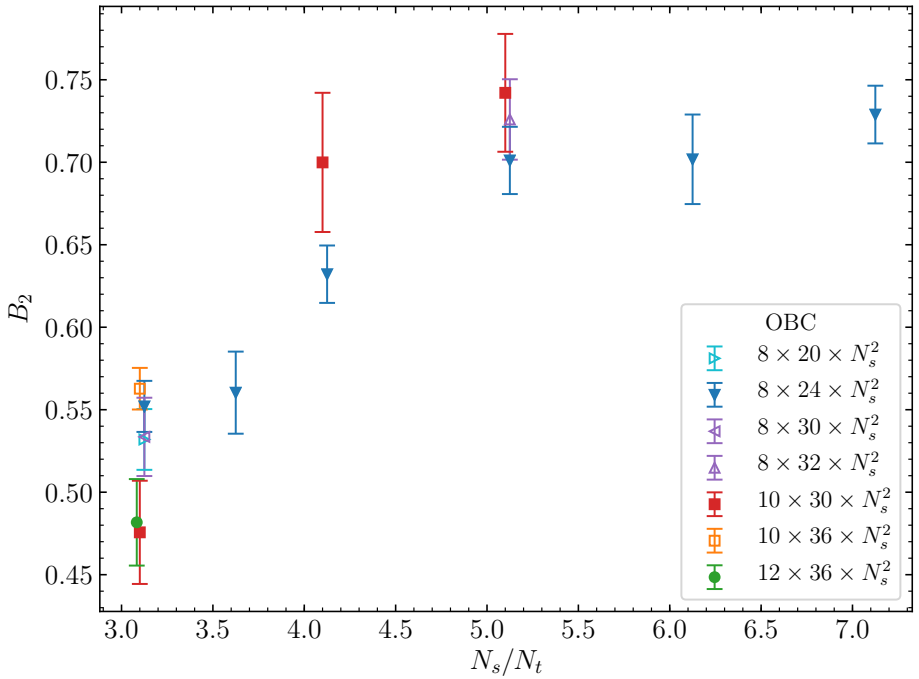

The linear velocity on the boundary $v_I = \Omega_I \, (N_s - 1) \, a(\beta_c)/2$

$$\frac{T_c(v_I)}{T_c(0)} = 1 - B_2 \frac{v_I^2}{c^2} \qquad \Longrightarrow \qquad \frac{T_c(v)}{T_c(0)} = 1 + B_2 \frac{v^2}{c^2}$$

- The critical temperature increases with the angular velocity.
- The coefficient B_2 slightly depends on the transverse lattice size (N_s/N_t), but almost independent of both the lattice spacing and the lattice size along the rotation axis (N_z/N_t).
- For lattices with sufficiently large N_s and OBC the coefficient is $B_2 \simeq 0.7$.

Rotating gluodynamics: Periodic boundary conditions

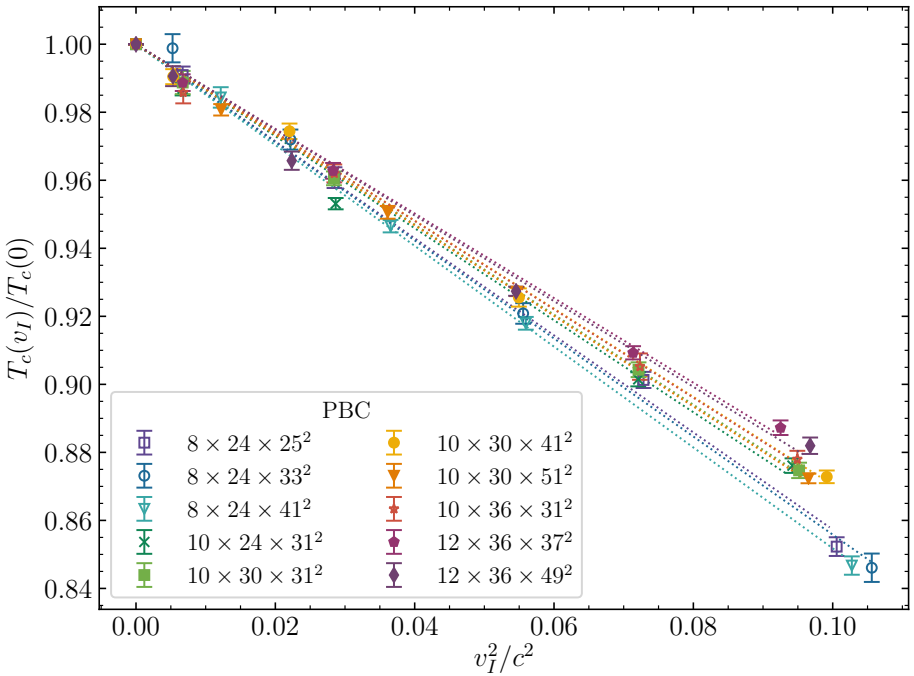

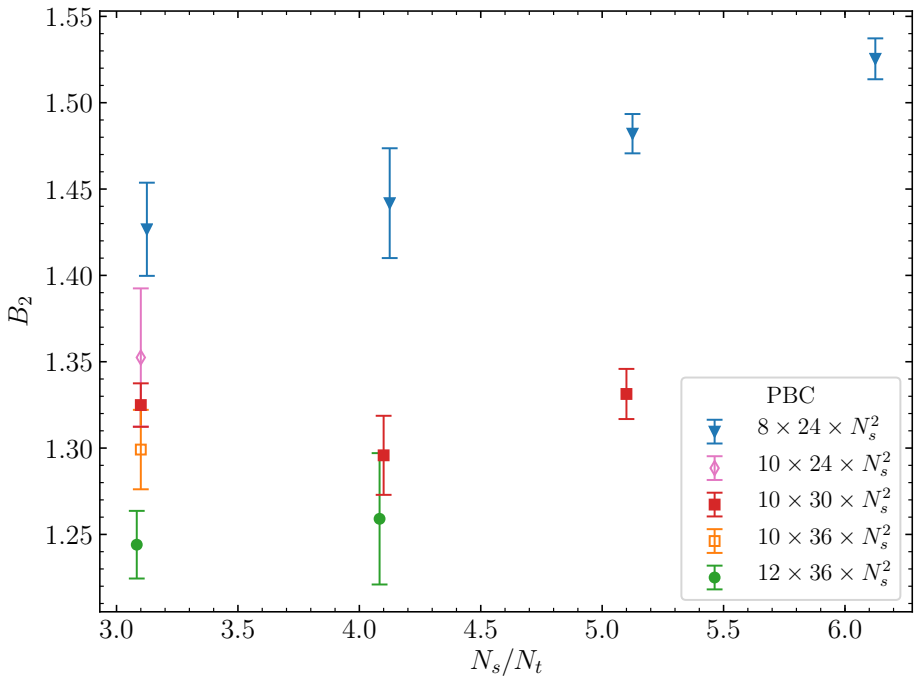

The linear velocity on the boundary $v_I = \Omega_I \, (N_s - 1) \, a(\beta_c)/2$

$$\frac{T_c(v_I)}{T_c(0)} = 1 - B_2 \frac{v_I^2}{c^2} \qquad \Longrightarrow \qquad \frac{T_c(v)}{T_c(0)} = 1 + B_2 \frac{v^2}{c^2}$$

- The critical temperature increases with the angular velocity.
- The results for the finest lattices with $N_t = 10, 12$ are close to each others, and for PBC the coefficient is $B_2 \sim 1.3$.

Rotating gluodynamics: Dirichlet boundary conditions

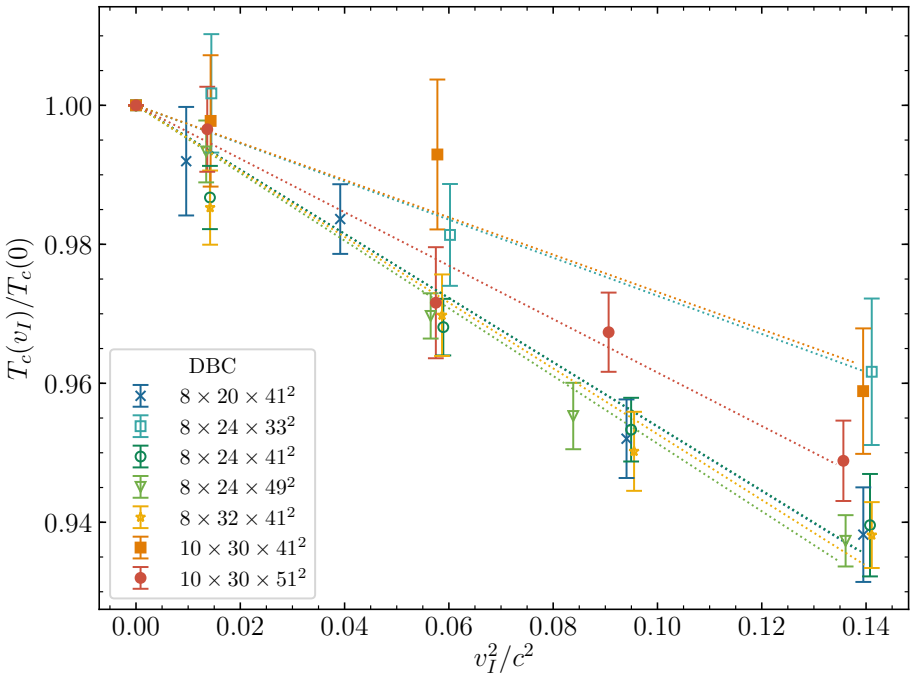

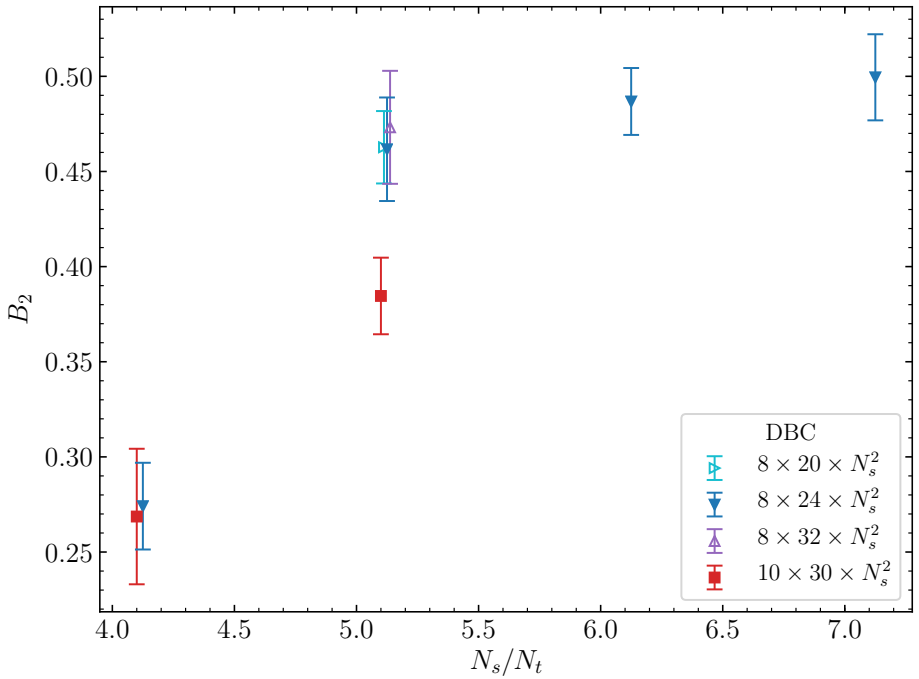

The linear velocity on the boundary $v_I = \Omega_I \, (N_s - 1) \, a(\beta_c)/2$

$$\frac{T_c(v_I)}{T_c(0)} = 1 - B_2 \frac{v_I^2}{c^2} \qquad \Longrightarrow \qquad \frac{T_c(v)}{T_c(0)} = 1 + B_2 \frac{v^2}{c^2}$$

- The critical temperature increases with the angular velocity.
- For lattices with sufficiently large N_s and DBC the coefficient goes to plateau $B_2 \sim 0.5$.

Rotation and susceptibility scaling

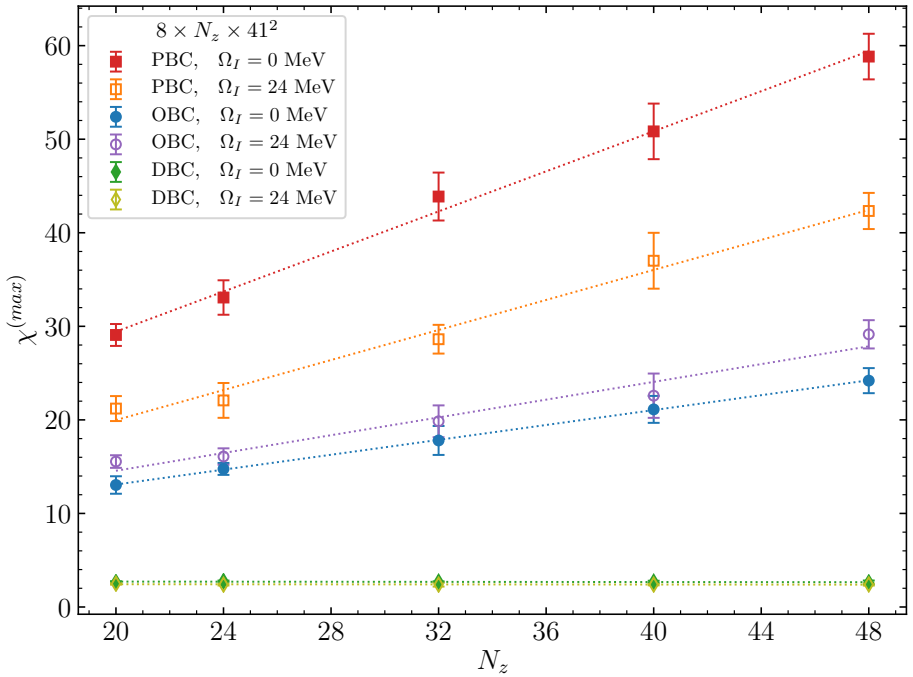

Figure: The height of the susceptibility peak for various lattices $8 \times N_z \times 41^2$ and zero/nonzero angular velocities.

Rotation does not change the order of the phase transition (in studied region of Ω):

- OBC: $\chi^{(max)} \sim V$
- PBC: $\chi^{(max)} \sim V$
- DBC: $\chi^{(max)} \sim const$

- Critical temperature in $N_f = 2$ QCD

Rotating QCD: lattice setup

- $N_f = 2$ clover-improved Wilson fermions (c_{SW} from one-loop) + RG-improved (Iwasaki) gauge action are used.
- "Replay" trick[3] is enabled to increase the stability of the HMC-algorithm.
- We reanalyze data for $m_{PS}a$ and $m_V a$ at zero temperature from CP-PACS and WHOT-QCD collaborations to restore LCP's more frequently in β and set the scale.
- The use of periodic/open/Dirichlet BC gives qualitatively the same results for rotating gluodynamics. PBC in directions x, y have been imposed.

[3] A. D. Kennedy, Nucl. Phys. B Proc. Suppl. **140**, edited by G. T. Bodwin et al., 190–203 (2005), arXiv:hep-lat/0409167.

Rotating QCD: lattice setup

- $N_f = 2$ clover-improved Wilson fermions (c_{SW} from one-loop) + RG-improved (Iwasaki) gauge action are used.
- "Replay" trick[3] is enabled to increase the stability of the HMC-algorithm.
- We reanalyze data for $m_{PS}a$ and $m_V a$ at zero temperature from CP-PACS and WHOT-QCD collaborations to restore LCP's more frequently in β and set the scale.
- The use of periodic/open/Dirichlet BC gives qualitatively the same results for rotating gluodynamics. PBC in directions x, y have been imposed.
- The critical temperature in gluodynamics depends mainly on the linear velocity on the boundary $v_I = \Omega_I (N_s - 1)a$. Thus, v_I is fixed in simulations instead of angular velocity Ω_I in physical units (e.g., MeV).
- Up to now, only results with $N_t = 4$ are available, work in progress...

[3] A. D. Kennedy, Nucl. Phys. B Proc. Suppl. **140**, edited by G. T. Bodwin et al., 190–203 (2005), arXiv:hep-lat/0409167.

Rotating QCD: LCP and scale setting

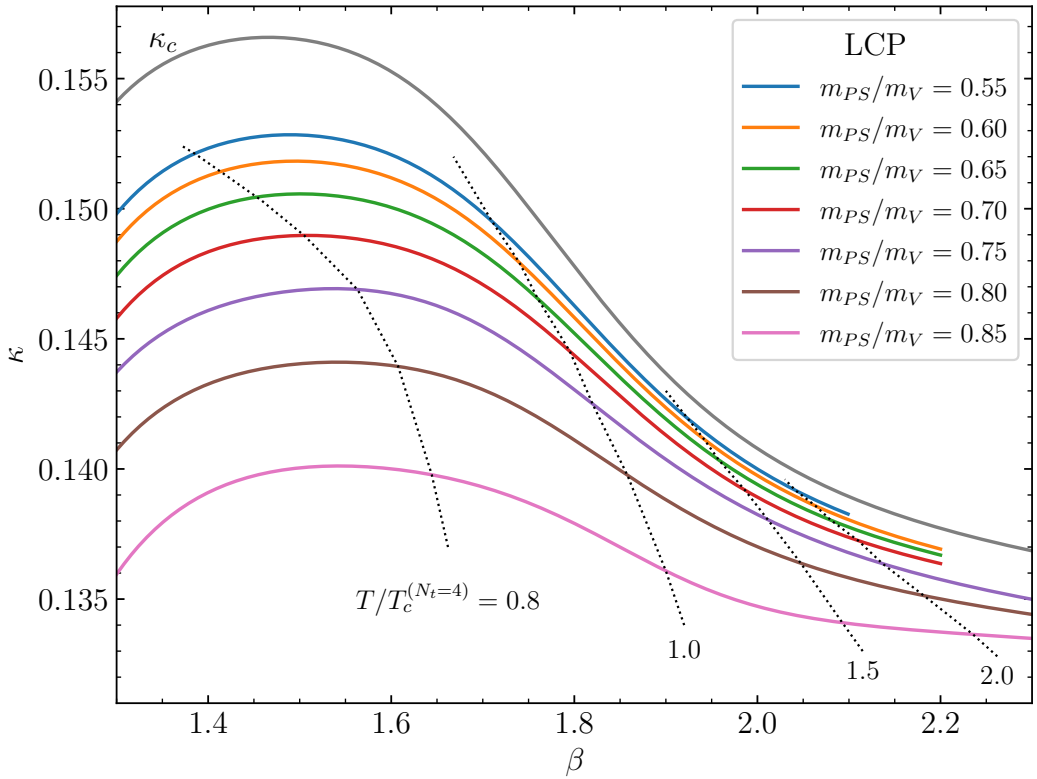

To set the temperature along the given LCP we use the zero-temperature mass of vector meson (m_V-input)

$$\frac{T}{m_V}(m_{PS}/m_V, \beta) = \frac{1}{N_t \times m_V a(m_{PS}/m_V, \beta)} \,. \tag{18}$$

and find

$$\frac{T}{T_{pc}}(\beta) = \frac{m_V a(\beta_{pc,\Omega=0})}{m_V a(\beta)}$$

The Polyakov loop is

$$L(\vec{x}) = \mathrm{Tr}\left[\prod_{\tau=0}^{N_t-1} U_4(\vec{x},\tau)\right], \qquad L = \frac{1}{N_s^2 N_z}\sum_{\vec{x}} L(\vec{x})\,. \tag{19}$$

The pseudo-critical temperature T_{pc} of the confinement/deconfinement phase transition is determined using the Polyakov loop susceptibility

$$\chi_L = N_s^2 N_z \left(\langle |L|^2 \rangle - \langle |L| \rangle^2\right), \tag{20}$$

by means of the Gaussian fit and as inflection point of Polyakov loop.

The (bare) chiral condensate is

$$\langle \bar{\psi}\psi \rangle^{bare} = -\frac{N_f T}{V}\left\langle \mathrm{Tr}(M^{-1})\right\rangle \tag{21}$$

For the chiral transition, pseudo-critical temperature T_{pc} is determined using peak of the (disconnected) chiral susceptibility:

$$\chi^{bare}_{\langle\bar{\psi}\psi\rangle} = \frac{N_f T}{V}\left[\left\langle \mathrm{Tr}(M^{-1})^2\right\rangle - \left\langle \mathrm{Tr}(M^{-1})\right\rangle^2\right] \tag{22}$$

Rotating QCD: Periodic boundary conditions

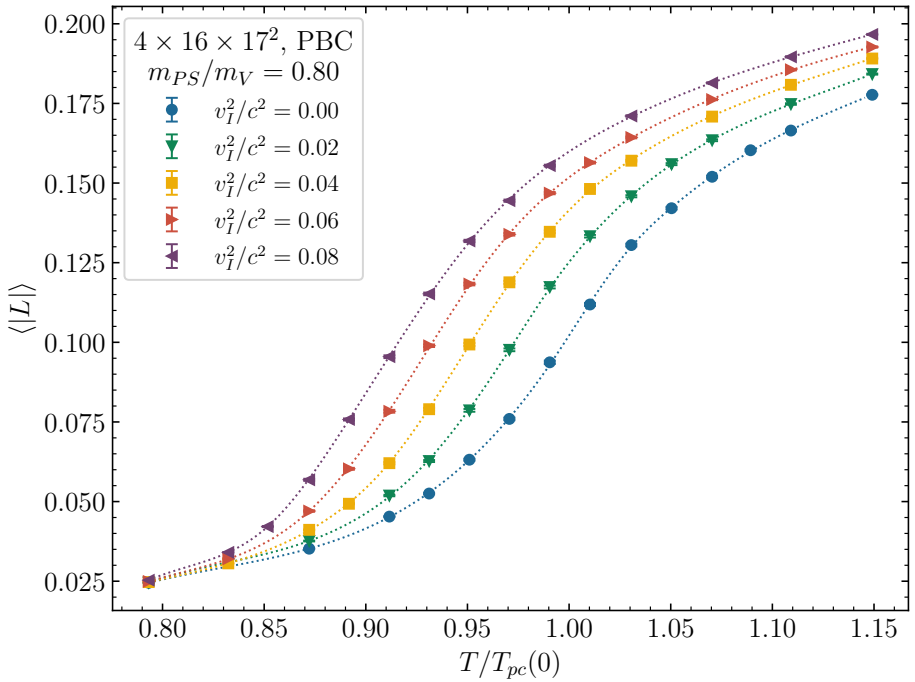

Figure: The Polyakov loop as a function of $T/T_{pc}(\Omega = 0)$ for different values of imaginary linear velocity on the boundary v_I. Lattice $4 \times 16 \times 17^2$, LCP $m_{PS}/m_V = 0.80$.

- Pseudo-critical temperature decreases due to imaginary rotation (same as in gluodynamics).

Rotating QCD: Periodic boundary conditions

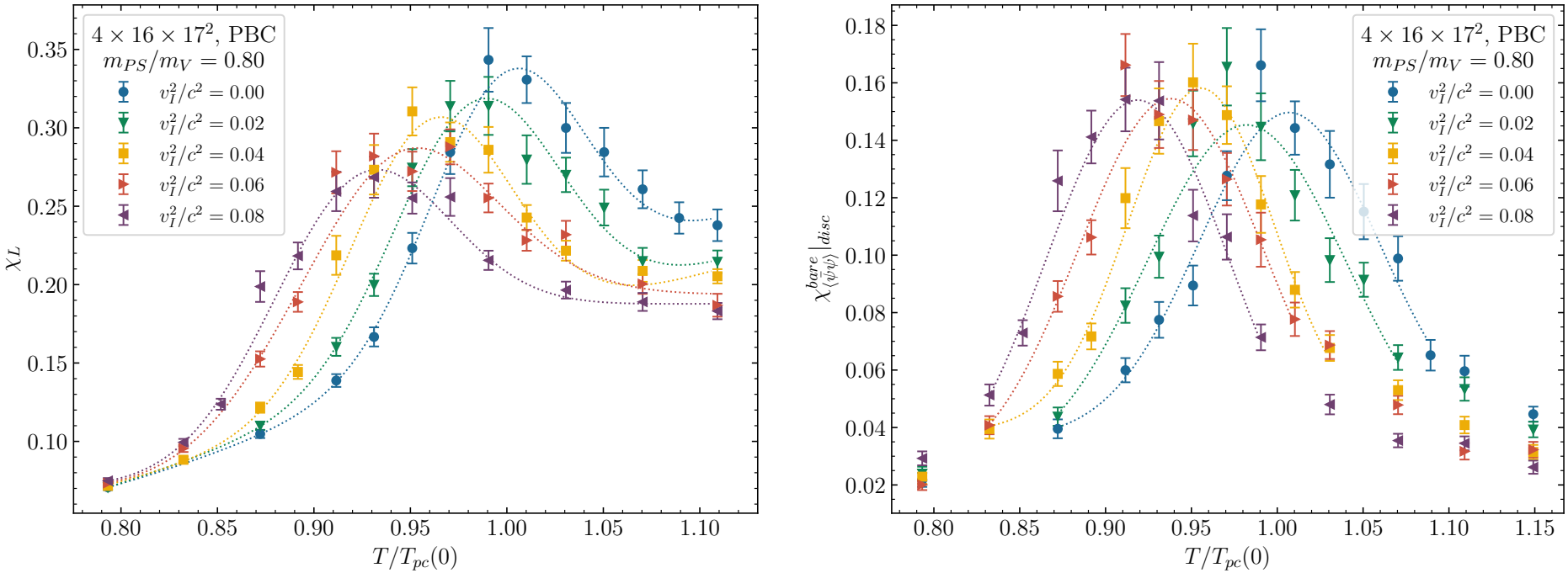

Figure: The Polyakov loop susceptibility and chiral susceptibility as a function of $T/T_{pc}(\Omega = 0)$ for different values of imaginary linear velocity on the boundary v_I. Lattice $4 \times 16 \times 17^2$, LCP $m_{PS}/m_V = 0.80$.

- Pseudo-critical temperature decreases due to imaginary rotation (same as in gluodynamics).

Rotating QCD: Periodic boundary conditions

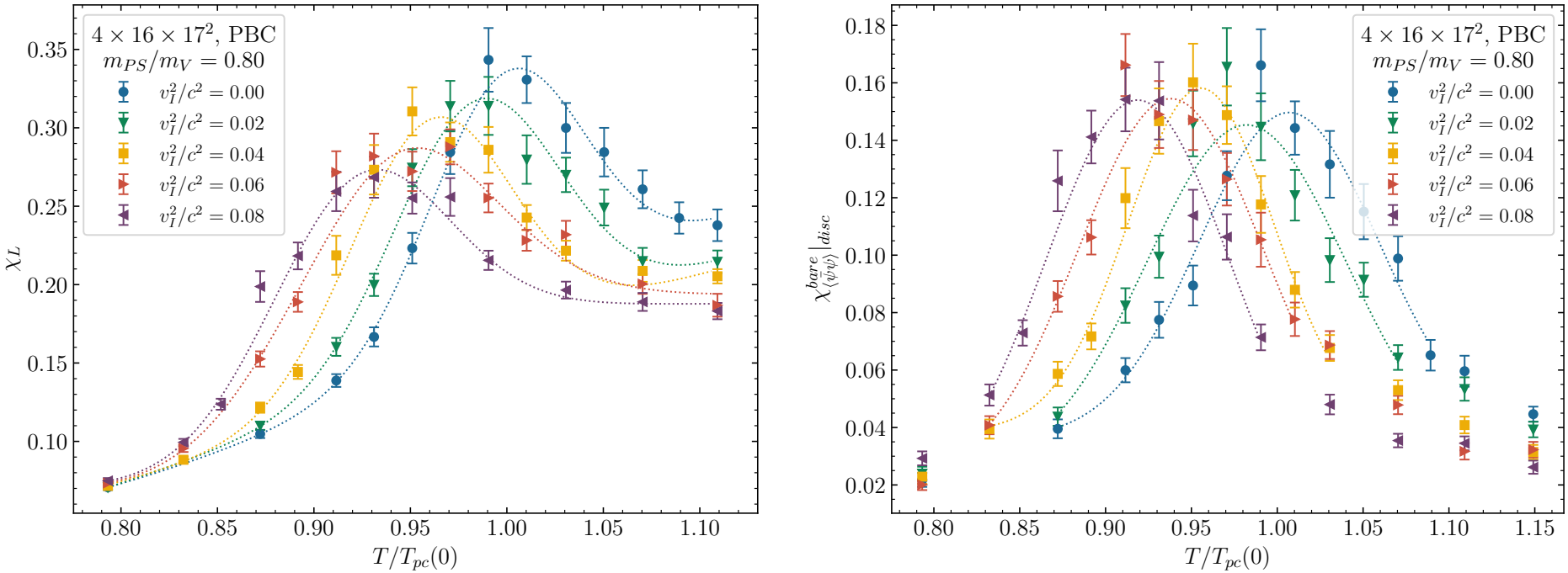

Figure: The Polyakov loop susceptibility and chiral susceptibility as a function of $T/T_{pc}(\Omega = 0)$ for different values of imaginary linear velocity on the boundary v_I. Lattice $4 \times 16 \times 17^2$, LCP $m_{PS}/m_V = 0.80$.

- Pseudo-critical temperature decreases due to imaginary rotation (same as in gluodynamics).

In order to disentangle the effect of the rotation on fermions and gluons, the separate angular velocities are introduced: $S_G(\Omega_G) + S_F(\Omega_F)$.

Rotating QCD: various rotation regimes

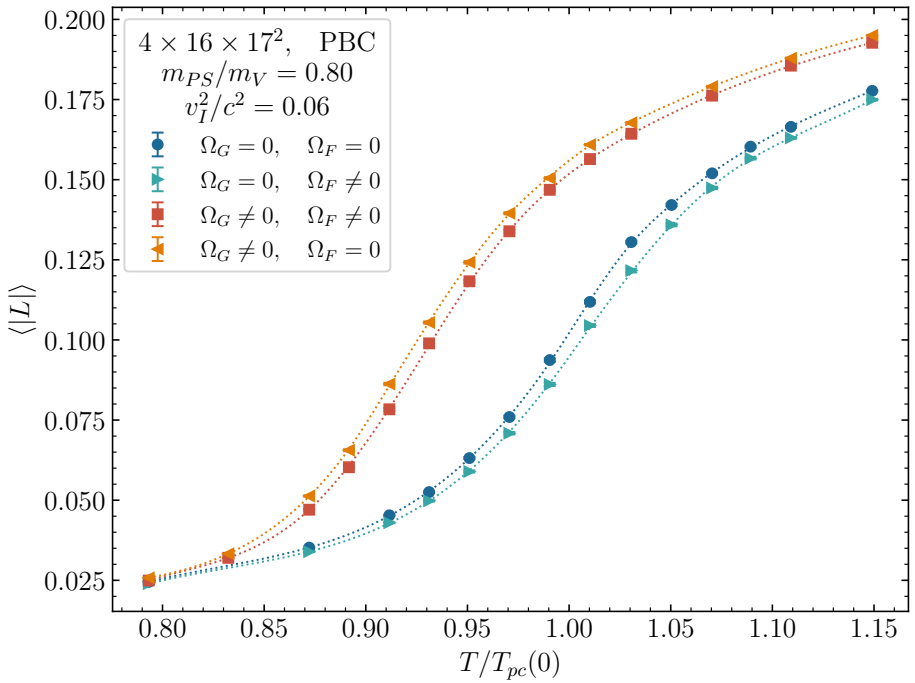

Figure: The Polyakov loop as a function of T/T_{pc} for various rotation regimes. Lattice $4 \times 16 \times 17^2$, $m_{PS}/m_V = 0.80$.

Rotating QCD: various rotation regimes

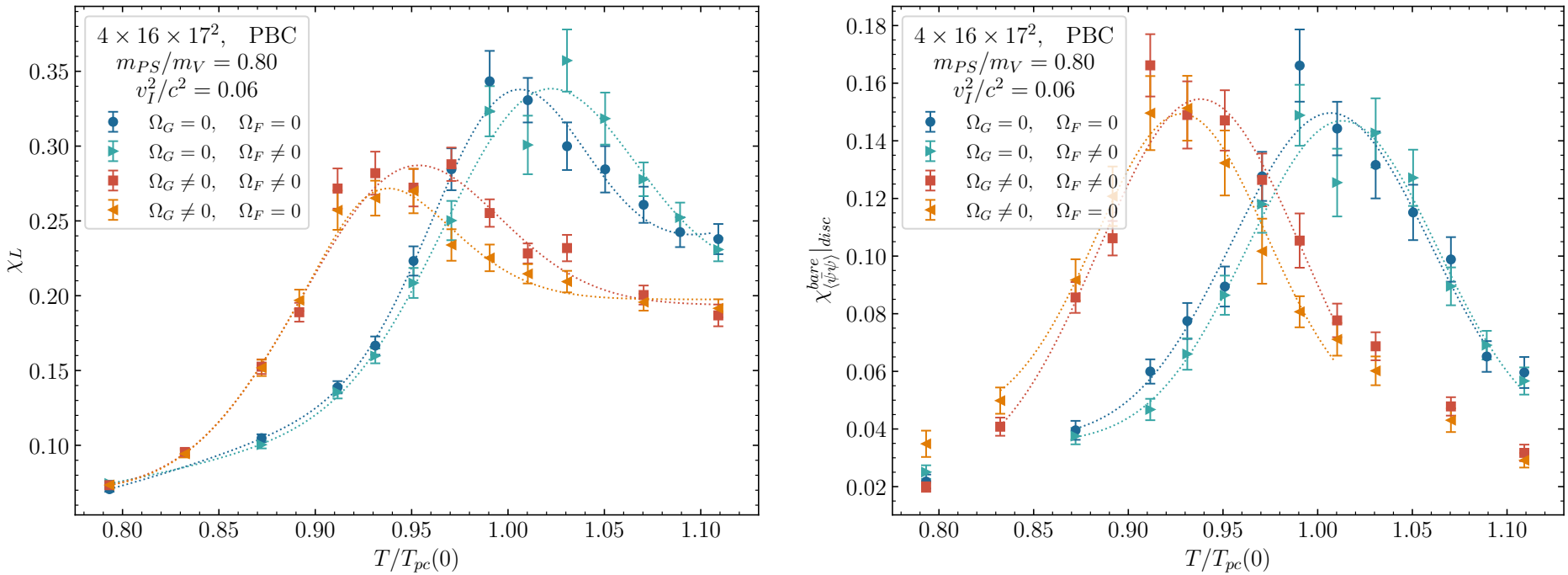

Figure: The Polyakov loop susceptibility and chiral susceptibility as a function of T/T_{pc} for various rotation regimes. Lattice $4 \times 16 \times 17^2$, $m_{PS}/m_V = 0.80$.

- Rotation of fermions and gluons separately has the opposite influence on the critical temperature.

Rotating QCD: various rotation regimes

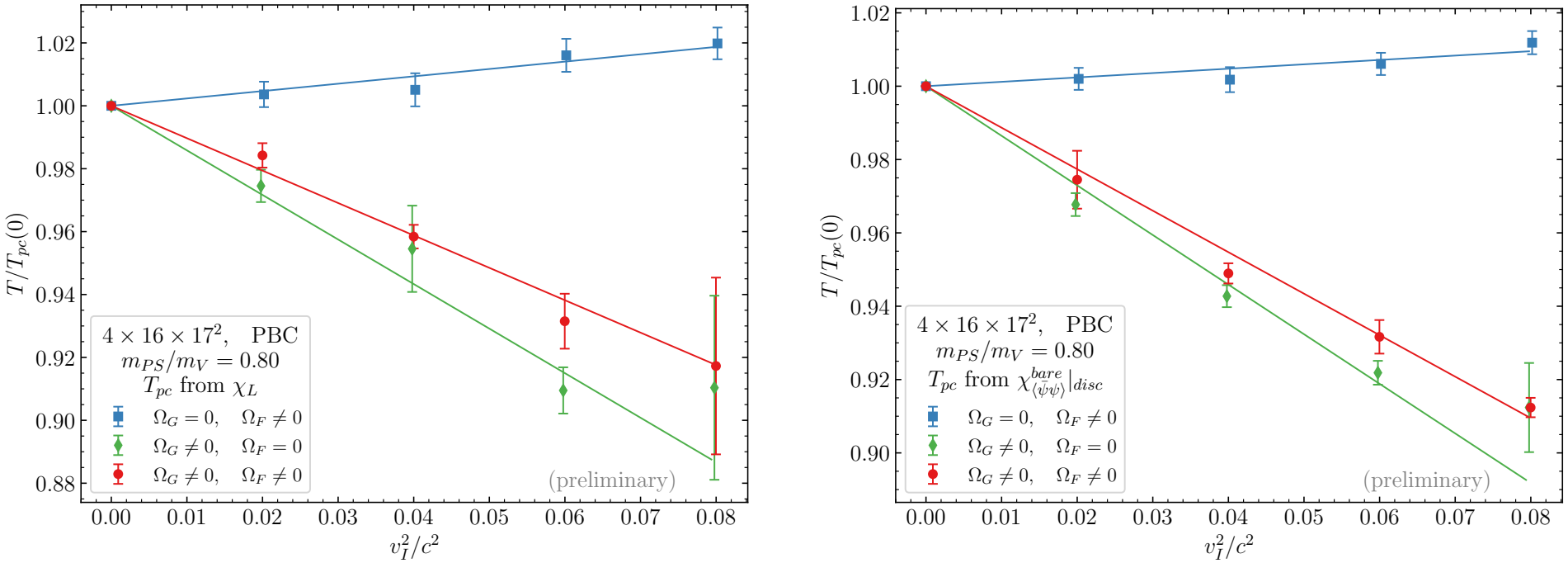

Figure: The pseudo-critical temperature as a function of imaginary linear velocity on the boundary for various rotation regimes (full, only gluons, only fermions).

$$\frac{T_{pc}(v_I)}{T_{pc}(0)} = 1 - B_2 \frac{v_I^2}{c^2} \tag{23}$$

$\Omega_G = \Omega_F \neq 0$	$\Omega_G \neq 0$	$\Omega_F \neq 0$
$B_2 > 0$	$B_2^{(G)} > B_2$	$B_2^{(F)} < 0$

Rotating QCD: various rotation regimes

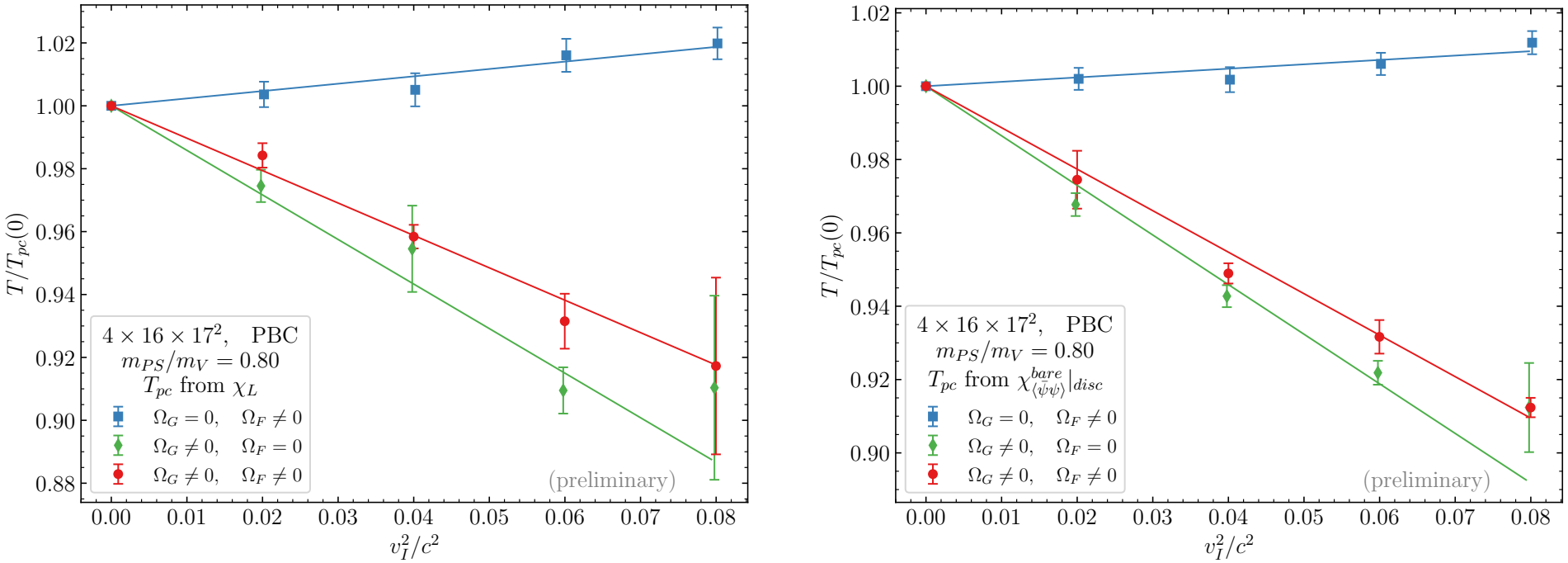

Figure: The pseudo-critical temperature as a function of imaginary linear velocity on the boundary for various rotation regimes (full, only gluons, only fermions).

$$\frac{T_{pc}(v_I)}{T_{pc}(0)} = 1 - B_2 \frac{v_I^2}{c^2} \tag{23}$$

$\Omega_G = \Omega_F \neq 0$	$\Omega_G \neq 0$	$\Omega_F \neq 0$
$B_2 > 0$	$B_2^{(G)} > B_2$	$B_2^{(F)} < 0$

How do the results depend on m_{PS}/m_V?

Rotating QCD: critical temperature

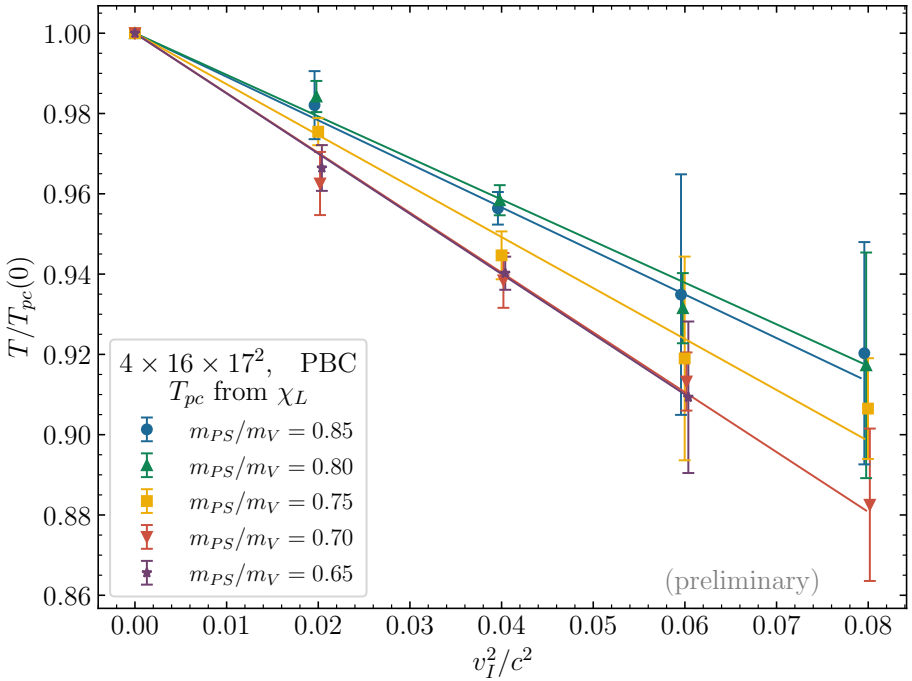

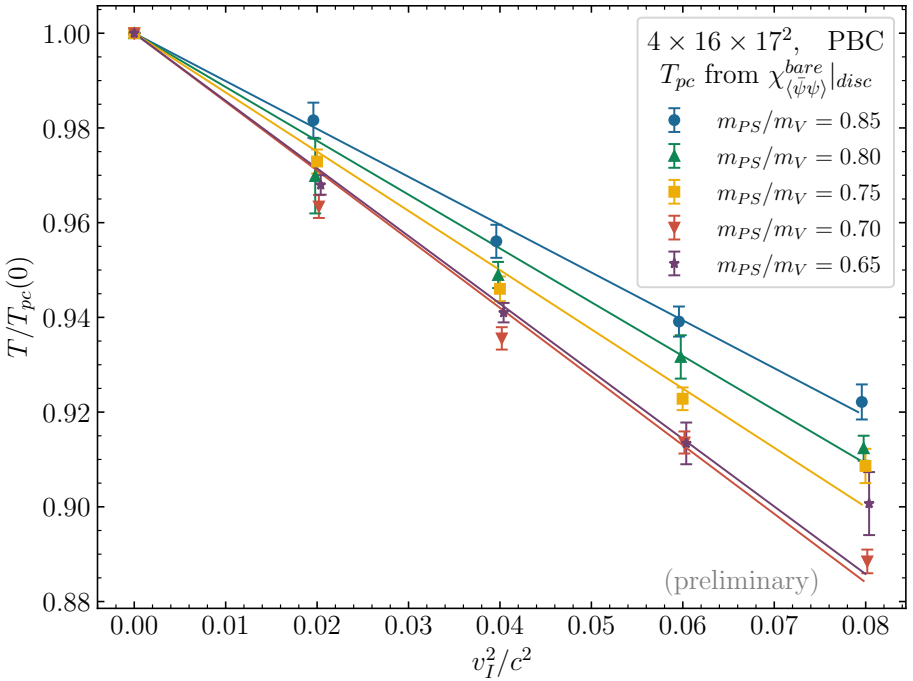

LCP's with $m_{PS}/m_V = 0.65, 0.70, 0.75, 0.80, 0.85$ were considered; $v_I/c < 0.3$.

$$\frac{T_{pc}(v_I)}{T_{pc}(0)} = 1 - B_2 \frac{v_I^2}{c^2}$$

Rotating QCD: critical temperature

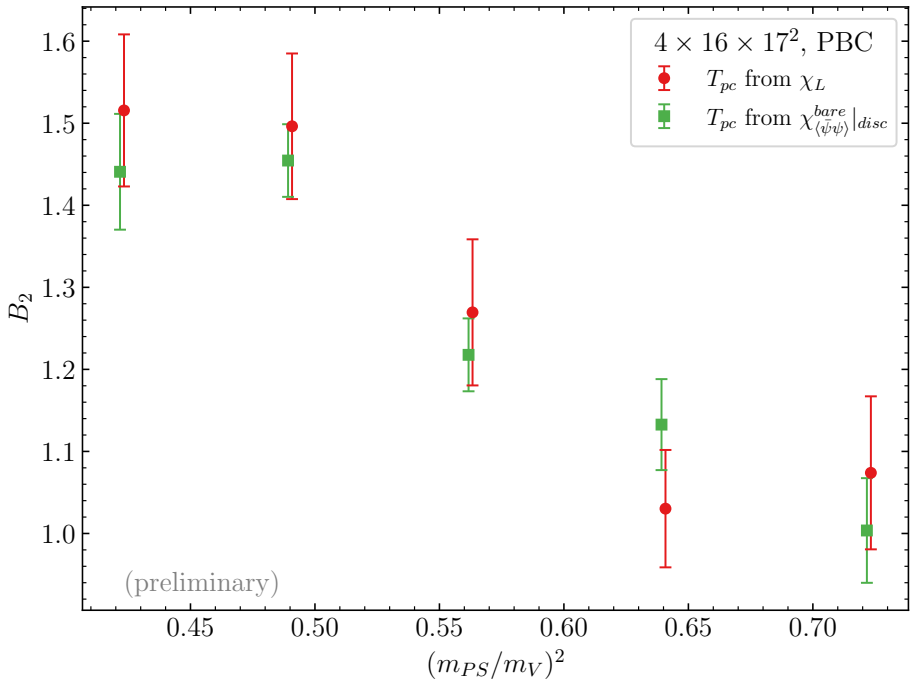

LCP's with $m_{PS}/m_V = 0.65, 0.70, 0.75, 0.80, 0.85$ were considered; $v_I/c < 0.3$.

$$\frac{T_{pc}(v_I)}{T_{pc}(0)} = 1 - B_2 \frac{v_I^2}{c^2} \qquad \Longrightarrow \qquad \frac{T_{pc}(v)}{T_{pc}(0)} = 1 + B_2 \frac{v^2}{c^2}$$

- The pseudo-critical temperature increases with the angular velocity ($v \propto \Omega$).
- The coefficient B_2 slightly grows with decreasing pion mass in considered range.
- The chiral transition shifts to the same direction as confinement-deconfinement transition.

- Rotating gluodynamics: Polyakov loop distributions

Open boundary conditions: Polyakov loop distribution

The local Polyakov loop in x, y-plane

$$L(x,y) = \frac{1}{N_z} \sum_z L(x,y,z)$$

Open boundary conditions: Polyakov loop distribution

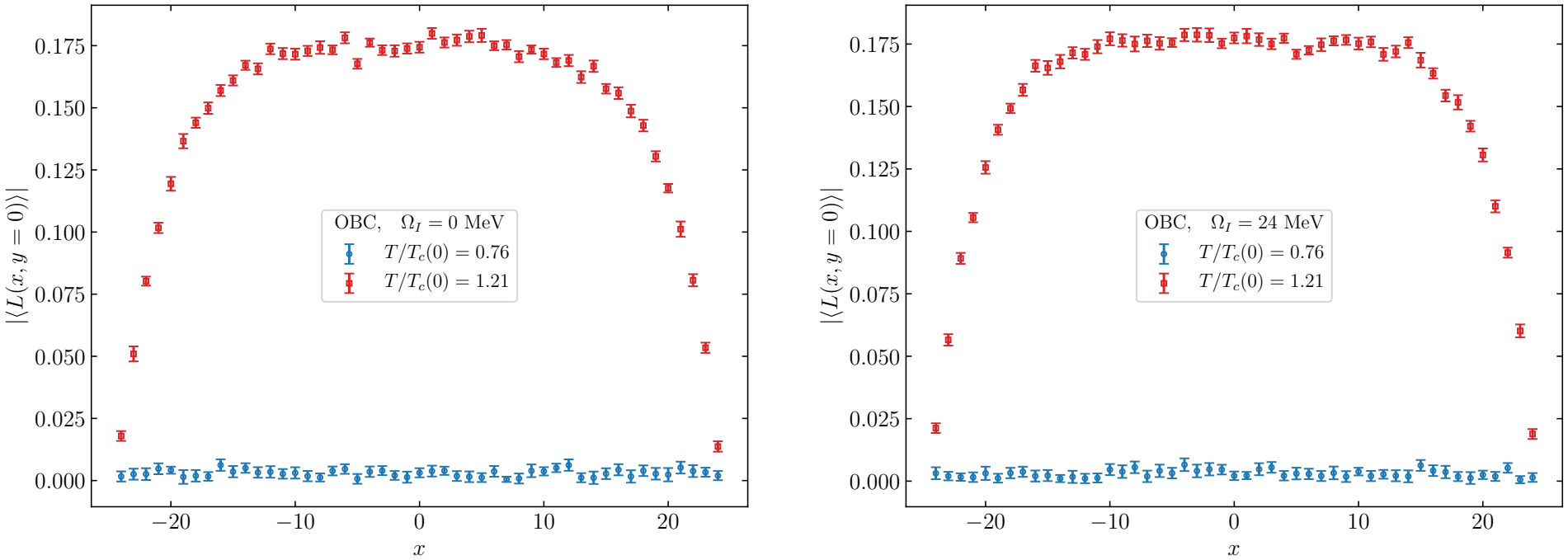

Figure: The local Polyakov loop $|\langle L(x, y)\rangle|$ as a function of coordinate for OBC and $\Omega_I = 0$ MeV (left), $\Omega_I = 24$ MeV (right). Points with $x \neq 0, y = 0$ from the lattice $8 \times 24 \times 49^2$ are shown.

- The local Polyakov loop $|\langle L(x, y)\rangle|$ is zero for all spatial points in the confinement phase, both with and without rotation $\Rightarrow$ Polyakov loop still acts as the order parameter.
- In deconfinement phase the boundary is screened.

Periodic boundary conditions: Polyakov loop distribution

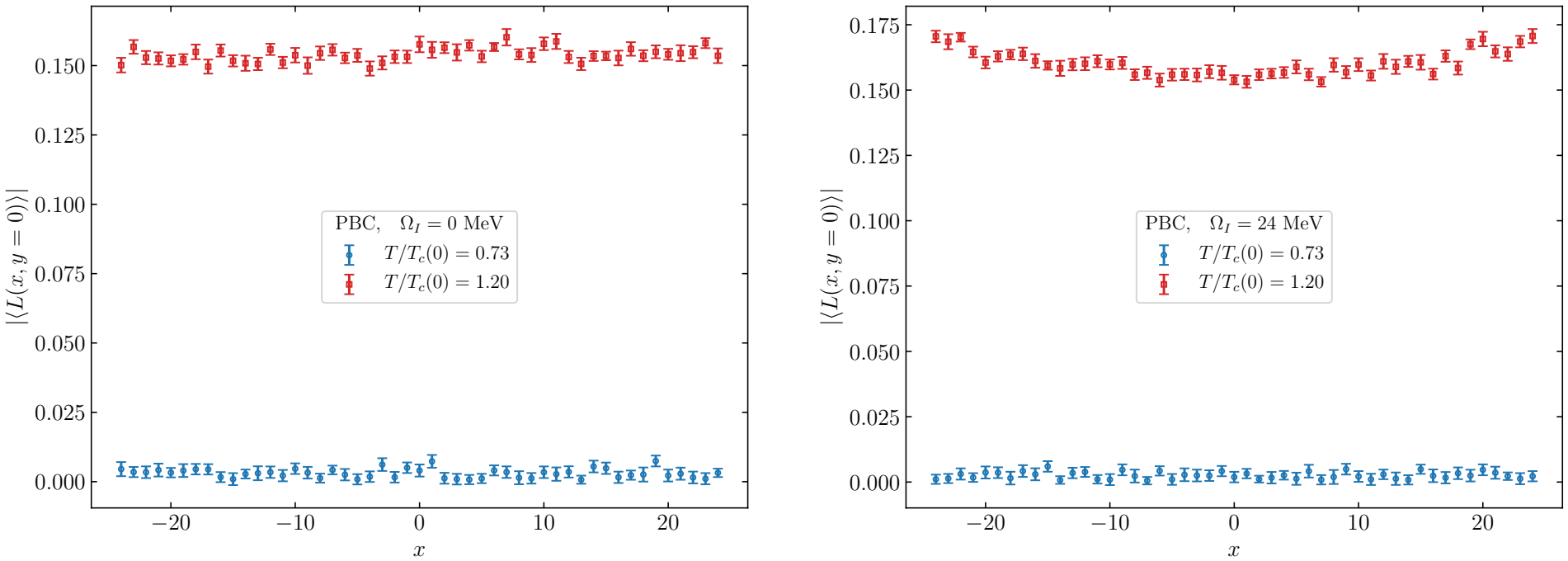

Figure: The local Polyakov loop $|\langle L(x, y)\rangle|$ as a function of coordinate for OBC and $\Omega_I = 0$ MeV (left), $\Omega_I = 24$ MeV (right). Points with $x \neq 0, y = 0$ from the lattice $8 \times 24 \times 49^2$ are shown.

- The local Polyakov loop $|\langle L(x, y)\rangle|$ is zero for all spatial points in the confinement phase, both without rotation and with nonzero angular velocity.
- The local Polyakov loop demonstrates weak dependence on the coordinate in the deconfinement phase.

Dirichlet boundary conditions: Polyakov loop distribution

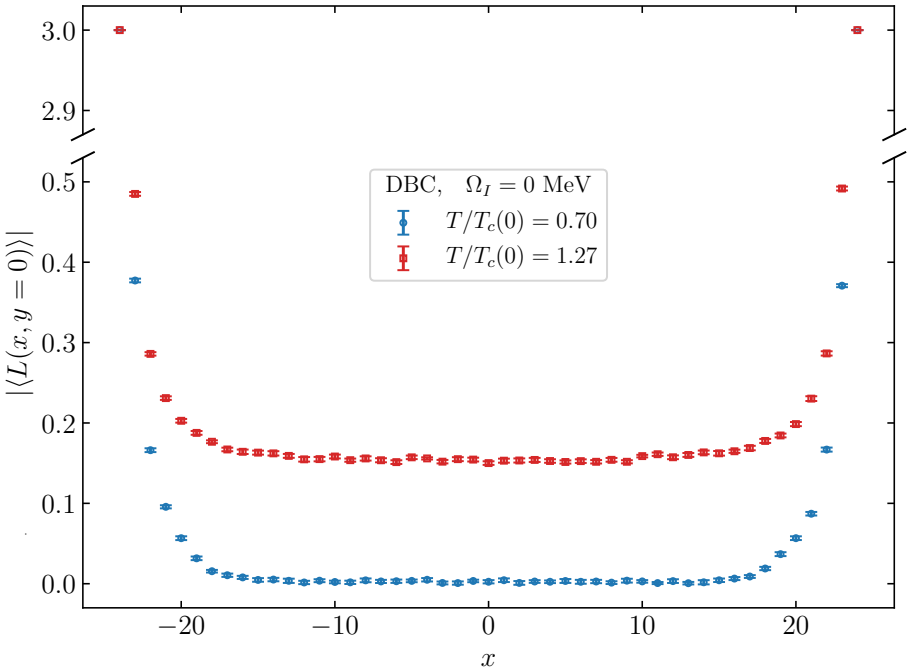

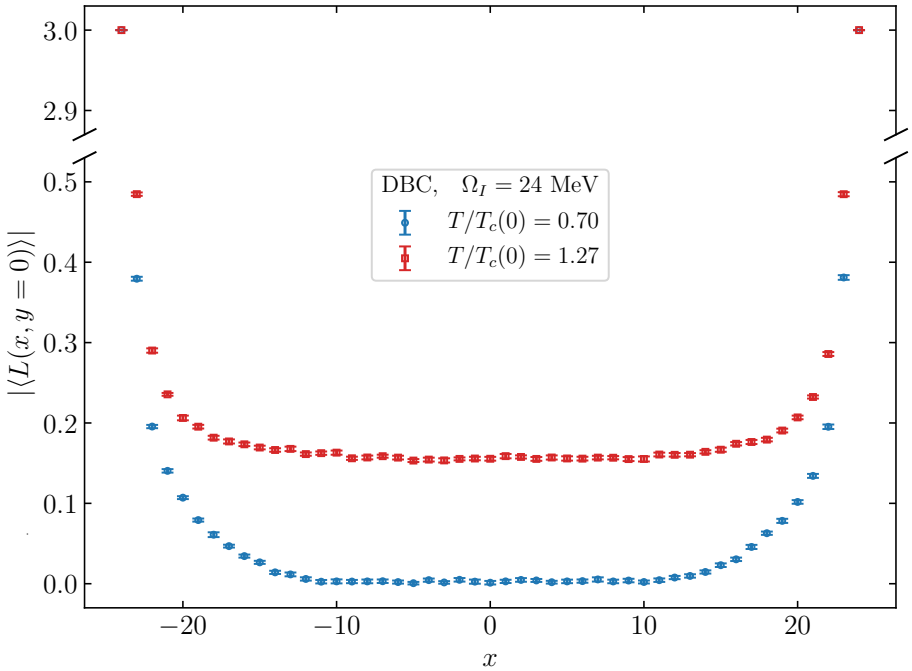

Figure: The local Polyakov loop $|\langle L(x, y)\rangle|$ as a function of coordinate for OBC and $\Omega_I = 0$ MeV (left), $\Omega_I = 24$ MeV (right). Points with $x \neq 0, y = 0$ from the lattice $8 \times 24 \times 49^2$ are shown.

- The local Polyakov loop $|\langle L(x, y)\rangle|$ is equal three on the boundary in both phases.
- The boundary is screened.

Open/Periodic boundary conditions: inhomogeneous phases?

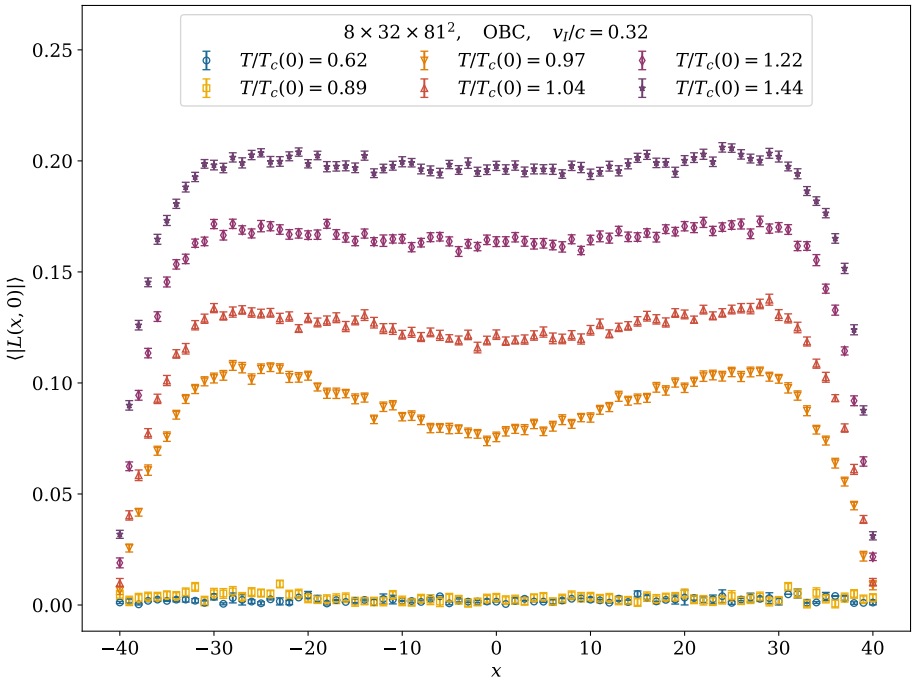

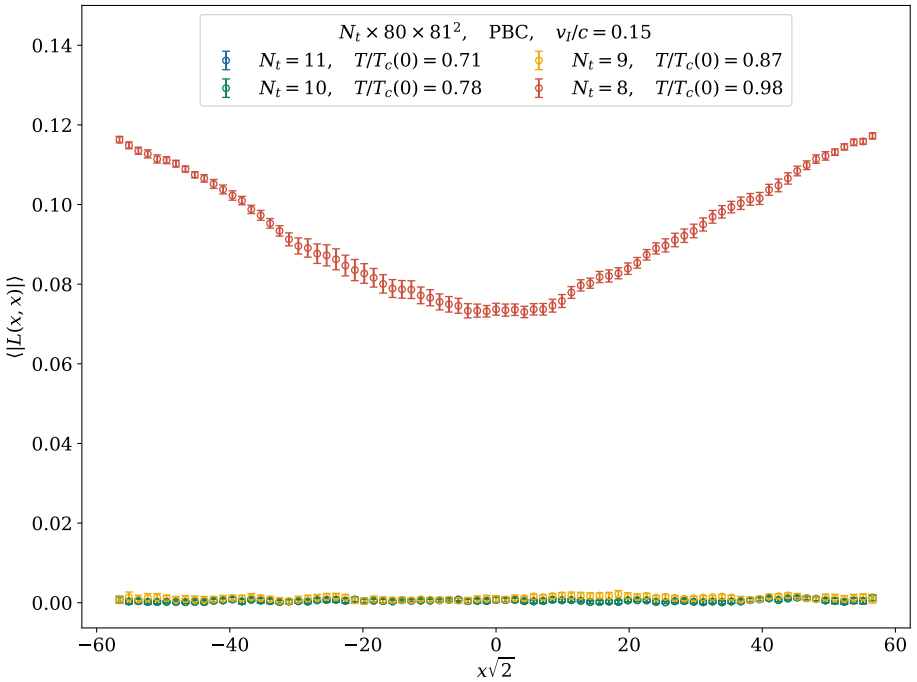

Figure: The local Polyakov loop $|\langle L(x,y)\rangle|$ as a function of coordinate for OBC/PBC (preliminary!).

- We need lattices with large spatial size.

Open/Periodic boundary conditions: inhomogeneous phases?

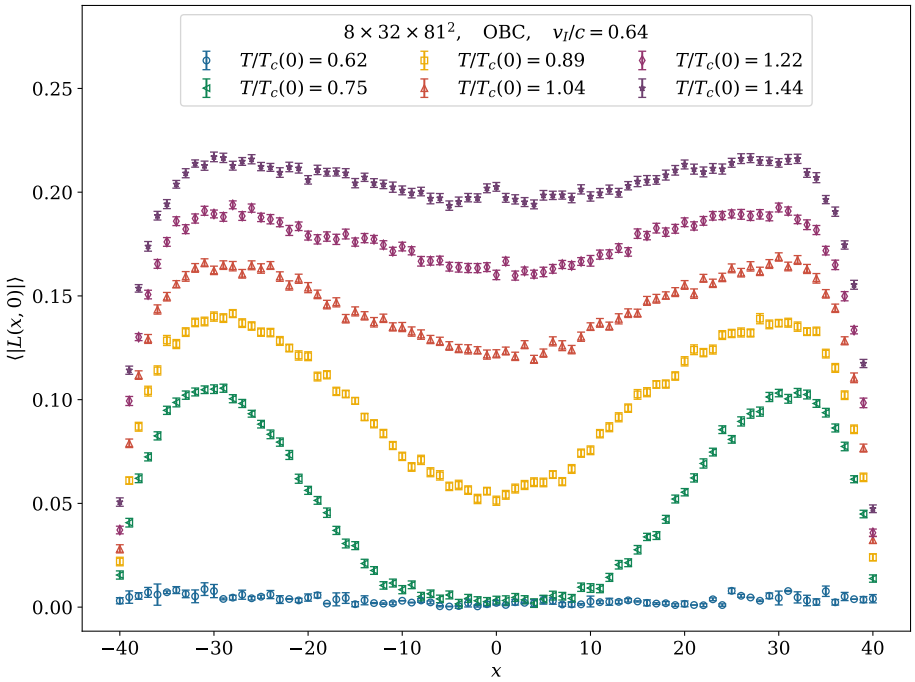

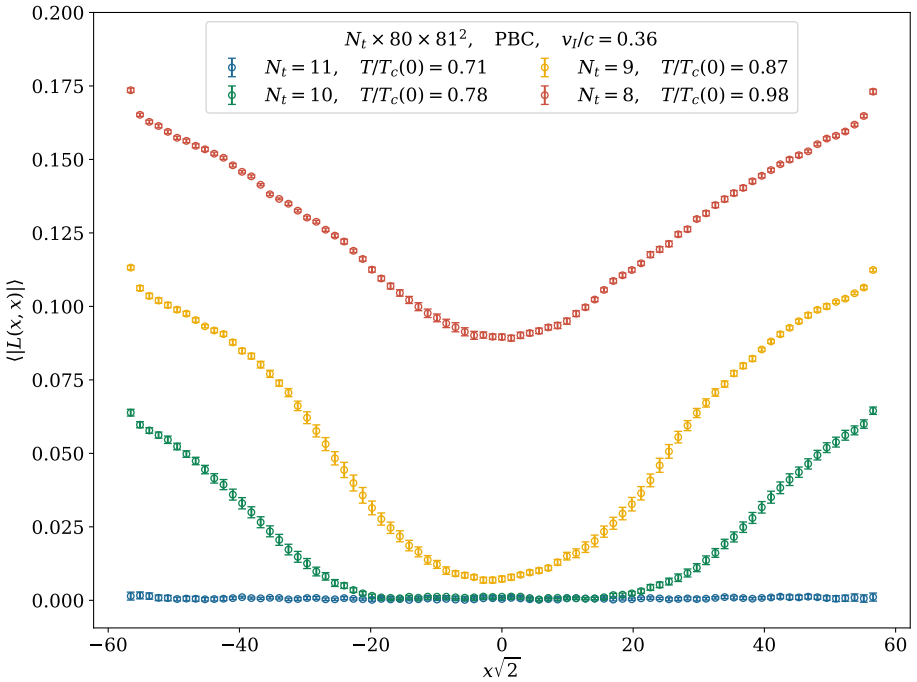

Figure: The local Polyakov loop $|\langle L(x,y)\rangle|$ as a function of coordinate for OBC/PBC (preliminary!).

- We need lattices with large spatial size.
- Confinement in center/Deconfinement on the periphery (imaginary rotation)?

Open/Periodic boundary conditions: inhomogeneous phases?

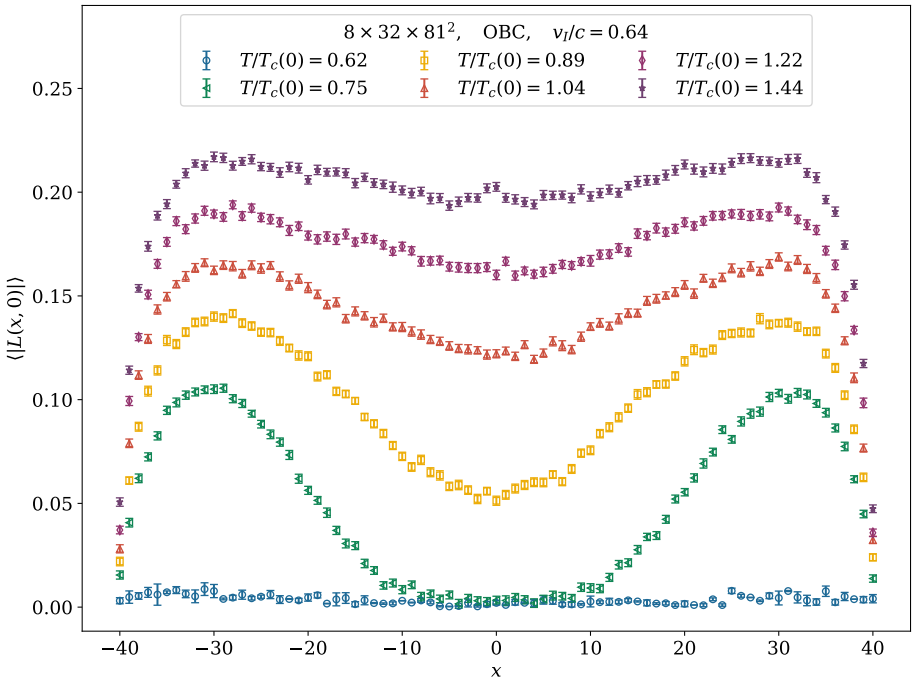

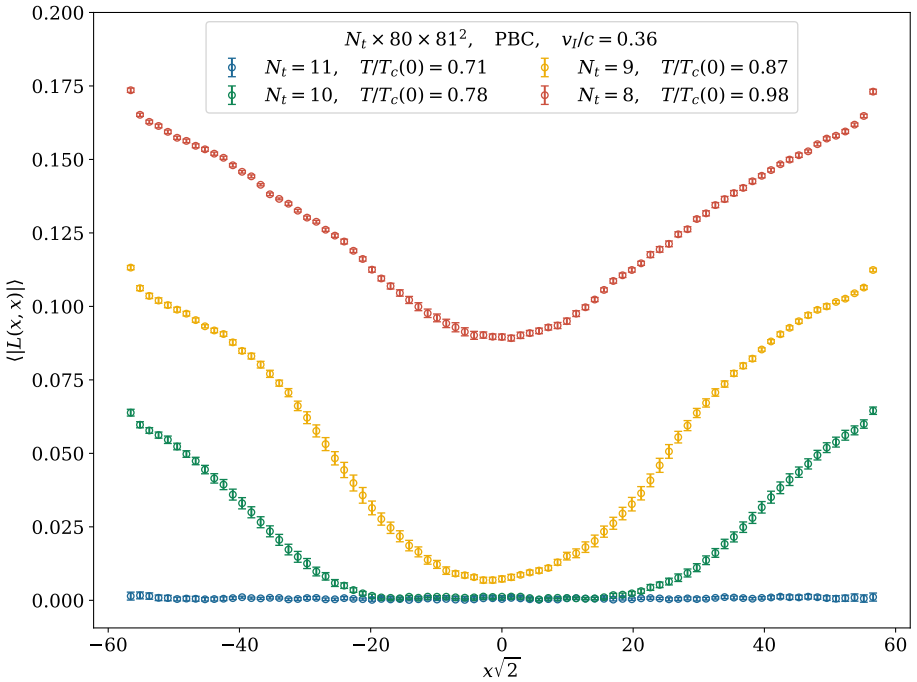

Figure: The local Polyakov loop $|\langle L(x,y)\rangle|$ as a function of coordinate for OBC/PBC (preliminary!).

- We need lattices with large spatial size.
- Confinement in center/Deconfinement on the periphery (imaginary rotation)?
- What happens in continuum limit?

- Rotating gluodynamics: Equation of State

All thermodynamic quantities can be derived from the partition function $Z(T, V)$. Its logarithm defines the free energy density

$$F = -T \ln Z$$

or

$$\frac{f}{T^4} = -\frac{1}{VT^3} \ln Z$$

We use standard integral method[4]:

$$\frac{f}{T^4}\Big|_{\beta_0}^{\beta} = -N_t^4 \int_{\beta_0}^{\beta} d\beta' \Big(\langle s \rangle_T - \langle s \rangle_0 \Big) \tag{24}$$

where

$$\langle s \rangle = -\frac{1}{N_t N_z N_s^2} \frac{\partial \ln Z}{\partial \beta} = \frac{1}{N_t N_z N_s^2} \langle S \rangle$$

[4] G. Boyd et al., Nucl. Phys. B **469**, 419–444 (1996), arXiv:hep-lat/9602007.

Rotating gluodynamics: Equation of State

- Gluon action: Wilson, Symanzik (in progress).
- Lattices: $N_t \times 40 \times 41^2$ and $40 \times 40 \times 41^2$.
- PBC, OBC (in progress).

Rotating gluodynamics: Equation of State

- Gluon action: Wilson, Symanzik (in progress).
- Lattices: $N_t \times 40 \times 41^2$ and $40 \times 40 \times 41^2$.
- PBC, OBC (in progress).

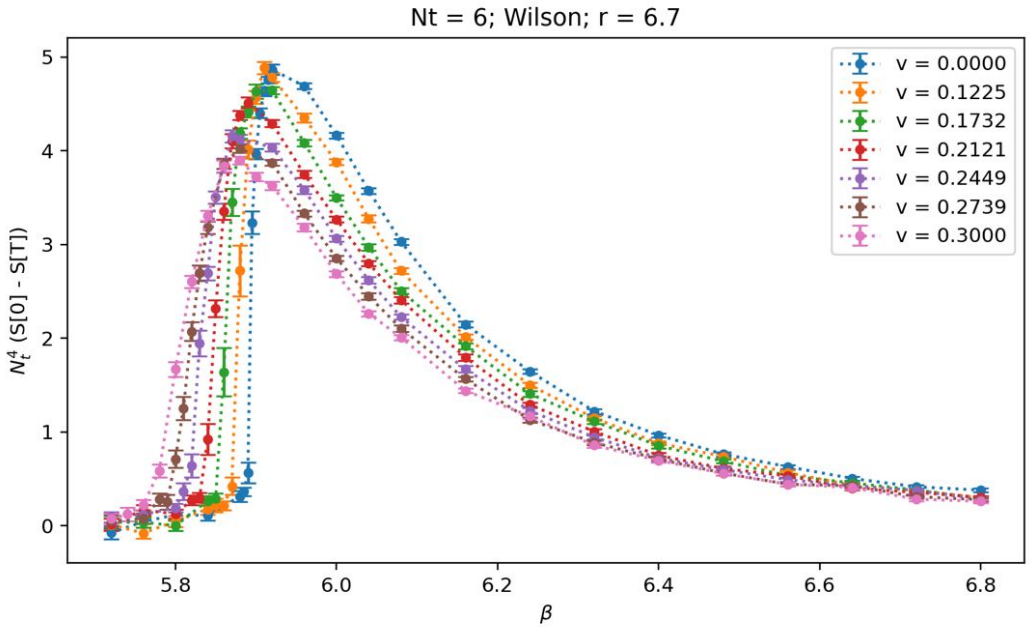

Figure: The difference $N_t^4(\langle s \rangle_{N_t=6} - \langle s \rangle_{N_t=40})$, PBC.

Free energy is measured in co-rotated reference frame and connected with values in the laboratory reference frame as follows[5]:

$$E = E^{(lab)} - J\Omega\,, \qquad dE = TdS + \cdots - Jd\Omega\,, \qquad dE^{(lab)} = TdS + \cdots + \Omega dJ\,,$$

and

$$F = E - TS\,, \qquad dF = -SdT + \cdots - Jd\Omega\,, \qquad dF^{(lab)} = -SdT + \cdots + \Omega dJ\,.$$

So, angular momentum is

$$J = I(\Omega)\,\Omega = -\left(\frac{\partial F}{\partial \Omega}\right)_T\,, \tag{25}$$

and

$$I(0) = -\left(\frac{\partial^2 F}{\partial \Omega^2}\right)_{T,\Omega=0}\,. \tag{26}$$

[5] M. Chernodub and S. Gongyo, JHEP **01**, 136 (2017), arXiv:1611.02598 [hep-th], L. D. Landau and E. M. Lifshitz, Vol. 5, Course of Theoretical Physics (Butterworth-Heinemann, Oxford, 1980).

Rotating gluodynamics: Equation of State

One can represent free energy as

$$\frac{f(\Omega_I) - f(0)}{T^4} = -\kappa_2 \Omega_I^2 + \kappa_4 \Omega_I^4 + \dots \tag{27}$$

Rotating gluodynamics: Equation of State

One can represent free energy as

$$\frac{f(v_I) - f(0)}{T^4} = -c_2 v_I^2 + c_4 v_I^4 + \dots \tag{27}$$

Rotating gluodynamics: Equation of State

One can represent free energy as

$$\frac{f(v) - f(0)}{T^4} = c_2 v^2 + c_4 v^4 + \dots \tag{27}$$

After analytical continuation

$$c_2 \longleftrightarrow -\frac{2I}{VT^4L^2}$$

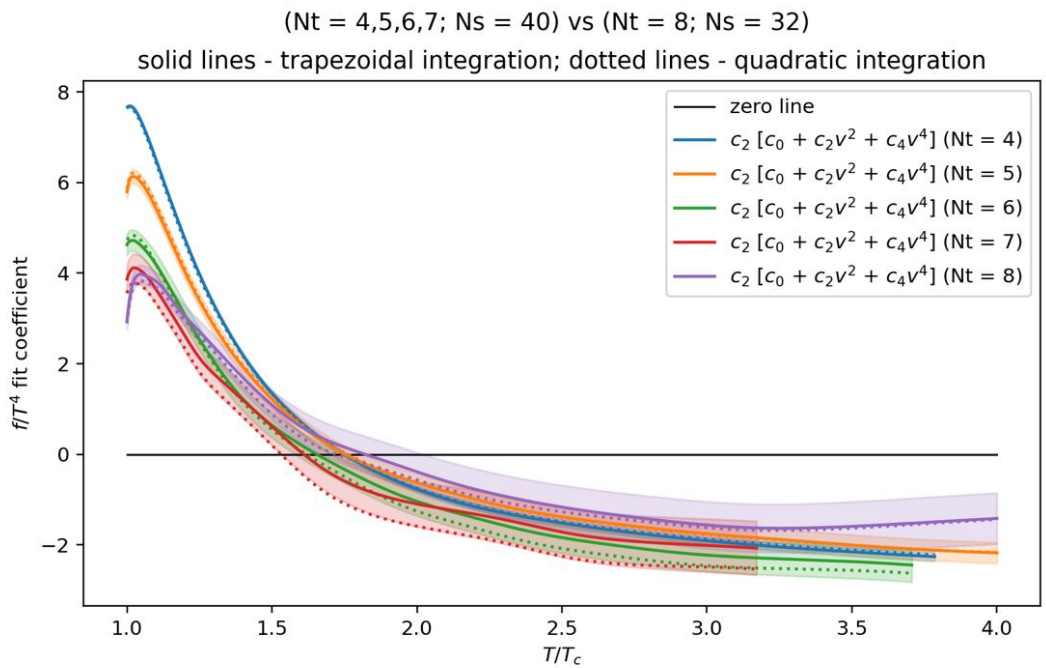

Figure: The coefficient c_2 from temperature, PBC. $c_2 = 0$ for $T \lesssim T_c$ (preliminary!).

Rotating gluodynamics: Moment of inertia

The coefficient c_2 ($-$ "thermal" part of the moment of inertia) has a contribution from magnetic part of gluon condensate ($F_{ij}^2 \longleftrightarrow P_\sigma$).

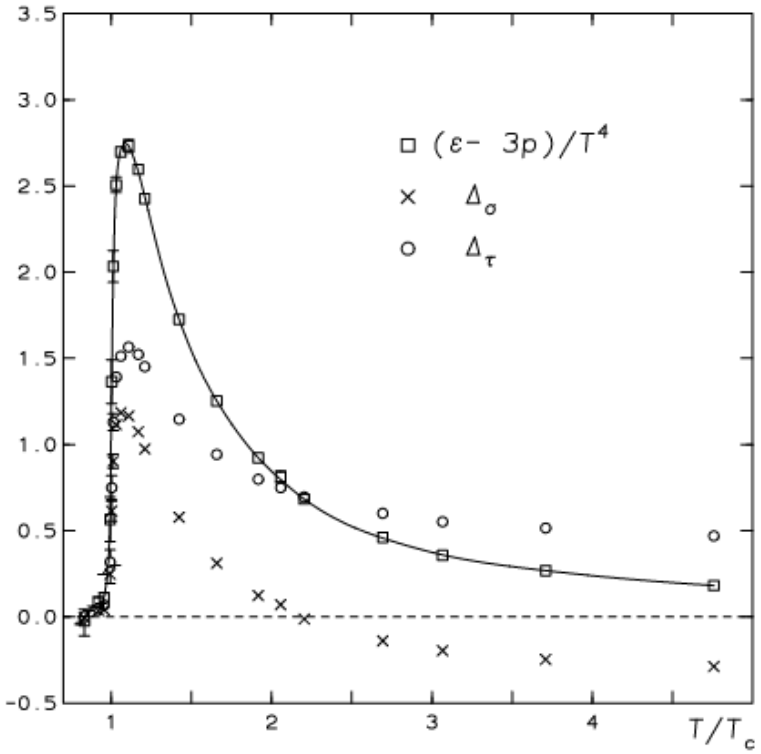

Figure 10: The space- and timelike components Δ_σ and Δ_τ of $(\epsilon - 3p)/T^4$ versus T/T_c on a $32^3 \times 6$ lattice.

Figure: From G. Boyd et al., Nucl. Phys. B **469**, 419–444 (1996), arXiv:hep-lat/9602007

Conclusions

- The critical temperature of the confinement/deconfinement transition in gluodynamics increases with angular velocity ($v \propto \Omega$)

$$\frac{T_c(v)}{T_c(0)} = 1 + B_2 \frac{v^2}{c^2} \, .$$

It's not Tolman-Ehrenfest effect!
(for OBC $B_2 \sim 0.7$, for PBC $B_2 \sim 1.3$ and for DBC $B_2 \sim 0.5$)

Conclusions

- The critical temperature of the confinement/deconfinement transition in gluodynamics increases with angular velocity ($v \propto \Omega$)

$$\frac{T_c(v)}{T_c(0)} = 1 + B_2 \frac{v^2}{c^2} \, .$$

  It's not Tolman-Ehrenfest effect!
  (for OBC $B_2 \sim 0.7$, for PBC $B_2 \sim 1.3$ and for DBC $B_2 \sim 0.5$)
- The separate rotation of quarks and gluons in QCD has the opposite influence on the critical temperature.
- The critical temperature in $N_f = 2$ QCD increases with angular velocity.
  (B_2 slightly grows with decreasing pion mass in range $m_{PS}/m_V = 0.65 \ \ldots \ 0.85$)

Conclusions

- The critical temperature of the confinement/deconfinement transition in gluodynamics increases with angular velocity ($v \propto \Omega$)

$$\frac{T_c(v)}{T_c(0)} = 1 + B_2 \frac{v^2}{c^2} \,.$$

  It's not Tolman-Ehrenfest effect!
  (for OBC $B_2 \sim 0.7$, for PBC $B_2 \sim 1.3$ and for DBC $B_2 \sim 0.5$)
- The separate rotation of quarks and gluons in QCD has the opposite influence on the critical temperature.
- The critical temperature in $N_f = 2$ QCD increases with angular velocity.
  (B_2 slightly grows with decreasing pion mass in range $m_{PS}/m_V = 0.65 \ \ldots \ 0.85$)
- It should be noted, that NJL (and other phenomenological models) predicts that critical temperature decreases due to the rotation. But taking into account the contribution of rotating gluons leads to an increase in T_c.

Conclusions

- The critical temperature of the confinement/deconfinement transition in gluodynamics increases with angular velocity ($v \propto \Omega$)

$$\frac{T_c(v)}{T_c(0)} = 1 + B_2 \frac{v^2}{c^2} \,.$$

  It's not Tolman-Ehrenfest effect!
  (for OBC $B_2 \sim 0.7$, for PBC $B_2 \sim 1.3$ and for DBC $B_2 \sim 0.5$)
- The separate rotation of quarks and gluons in QCD has the opposite influence on the critical temperature.
- The critical temperature in $N_f = 2$ QCD increases with angular velocity.
  (B_2 slightly grows with decreasing pion mass in range $m_{PS}/m_V = 0.65 \ \ldots \ 0.85$)
- It should be noted, that NJL (and other phenomenological models) predicts that critical temperature decreases due to the rotation. But taking into account the contribution of rotating gluons leads to an increase in T_c.
- Signs of the inhomogeneous phases are observed (imaginary rotation).

Conclusions

- The critical temperature of the confinement/deconfinement transition in gluodynamics increases with angular velocity ($v \propto \Omega$)

$$\frac{T_c(v)}{T_c(0)} = 1 + B_2 \frac{v^2}{c^2} \,.$$

  It's not Tolman-Ehrenfest effect!
  (for OBC $B_2 \sim 0.7$, for PBC $B_2 \sim 1.3$ and for DBC $B_2 \sim 0.5$)
- The separate rotation of quarks and gluons in QCD has the opposite influence on the critical temperature.
- The critical temperature in $N_f = 2$ QCD increases with angular velocity.
  (B_2 slightly grows with decreasing pion mass in range $m_{PS}/m_V = 0.65 \ \ldots \ 0.85$)
- It should be noted, that NJL (and other phenomenological models) predicts that critical temperature decreases due to the rotation. But taking into account the contribution of rotating gluons leads to an increase in T_c.
- Signs of the inhomogeneous phases are observed (imaginary rotation).
- Free energy of rotating gluodynamics becomes smaller in the vicinity of phase transition ($T/T_c \sim 1 - 1.5$) and increases for high temperature ($T/T_c > 2$).

- Work in progress... (but computing resources are limited)

Thank you for your attention!

See the details in:

- V. V. Braguta et al., JETP Lett. **112**, 6–12 (2020)
- N. Y. Astrakhantsev et al., Phys. Part. Nucl. **52**, 536–541 (2021)
- V. V. Braguta et al., Phys. Rev. D **103**, 094515 (2021), arXiv:2102.05084 [hep-lat]
- V. Braguta et al., PoS **LATTICE2021**, 125 (2022), arXiv:2110.12302 [hep-lat]
- arXiv: 2210. ...

Rotating NJL: Moment of inertia

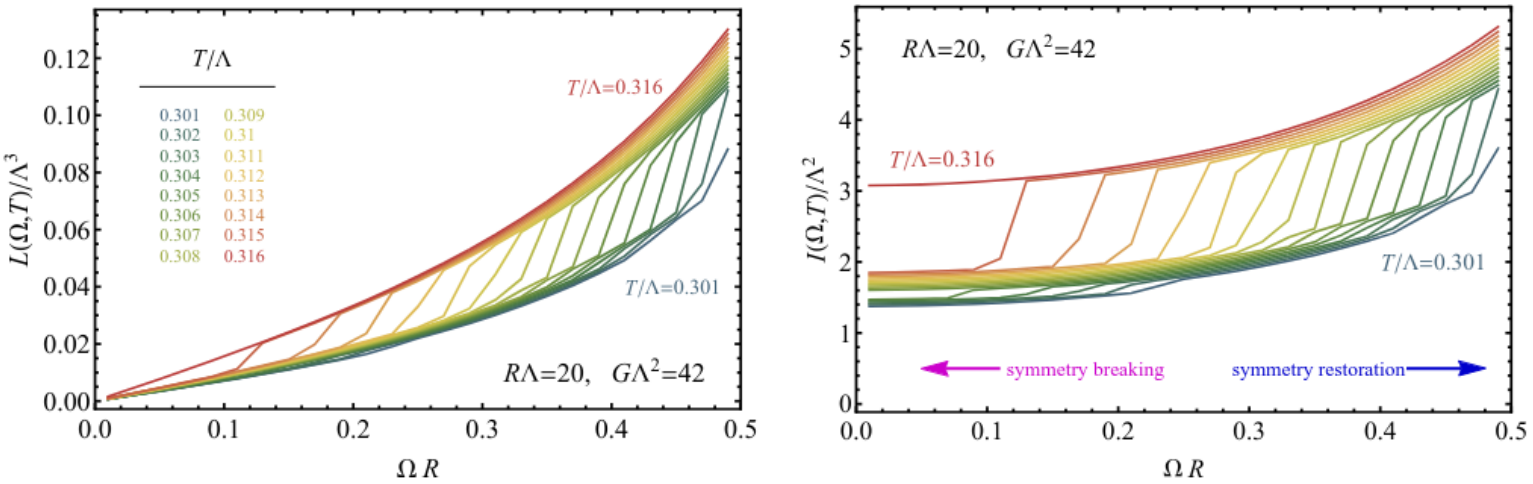

Figure 13. (a) The angular momentum (5.4) and (b) the moment of inertia (5.7) of the rotating fermionic matter across the phase transition line. The parameters are the same as in Fig. 12.

Figure: From M. Chernodub and S. Gongyo, JHEP **01**, 136 (2017), arXiv:1611.02598 [hep-th]